**Final Technical Report**

# ASHRAE Standard 152P Validation

## Basement Warm-Air Distribution Systems

**SYN TR 99-522**

**August 1999**

Synertech

Synertech Systems Corporation

Synertech

Synertech Systems Corporation

# Standard 152P Validation

Final Technical Report

Prepared for

**Brookhaven Science Associates, LLC**
P.O. Box 5000
Upton, L.I., NY 11973-5000

Contract No. 725097

Dr. John Andrews, Technical Representative

Prepared by

**SYNERTECH SYSTEMS CORPORATION**
Syracuse, New York 13202-2401

Peter R. Strunk
Ian M. Shapiro

August 1999

**118 Julian Place # 216 Syracuse, New York 13210-3419 315.446.2153 (V) 315.446.8844 (F)**

# TABLE OF CONTENTS

# TABLES

## FIGURES

# SUMMARY

This project investigated ASHRAE Standard 152P's accuracy in predicting the design and seasonal distribution efficiencies of five different configurations of a single residential warm-air thermal distribution system, as well as in predicting percentage differences in design and seasonal distribution efficiency between any two of the configurations. The configurations included different amounts of supply duct leakage, return duct leakage, and supply duct insulation levels.

Benchmark values for actual design and seasonal distribution efficiencies, obtained through independent field measurements, were compared with Standard 152P-predicted values. It was found that Standard 152P predicted lower distribution efficiencies for all five duct configurations. Further, Standard 152P predicted a significant change in distribution efficiency each time the ducts were re-configured, but the benchmark values were virtually unchanged through the first four duct configurations. Relatively large uncertainties for some of the configurations' benchmark results prevented extensive analysis of all differences between benchmark and Standard 152P values.

However, register flow measurements indicate that Standard 152P supply duct leakage flow values may be too high; in addition, thermal regain may be greater than the 0.5 value used in the Standard 152P calculations.

Importantly, both Standard 152P and benchmark values indicate that a substantial improvement in distribution efficiency is possible by insulating a basement duct system. Here the improvement was on the order of ten percent after the supply ducts were insulated.

# 1. Introduction

This project investigated ASHRAE Standard 152P's accuracy in predicting the design and seasonal distribution efficiencies of five different configurations of a single residential warm-air thermal distribution system, as well as in predicting percentage differences in design and seasonal distribution efficiency between any two of the configurations. The configurations included different amounts of supply duct leakage, return duct leakage, and supply duct insulation levels.

This testing of 152P's accuracy required benchmark values for actual design and seasonal distribution efficiencies, and benchmark values for actual percentage differences in design and seasonal efficiency. Once obtained, these values were compared with the 152P-predicted values to assess 152P's precision. All benchmark values were formed using independent field measurements, and the uncertainties of the eventual benchmarks range from 3.6 percent to 9.1 percent.

Importantly, each benchmark difference in distribution efficiency was not simply calculated from two benchmark absolute values, but was obtained using partially independent means that remove a source of error inherent in the absolute calculations.

Finally, calculating efficiencies using 152P required estimation of duct leakage. As part of the work, three variations of the House Pressure Test (HPT) method of estimating duct leakage (return-blocked, supply-blocked, and the newer hybrid test) were conducted to allow comparison of these methods with the duct pressurization method. This was done for each of the five duct configurations.

# 2. Methods

All field work was conducted in a vacant unfurnished single-family home with an unfinished basement, located in Syracuse, New York, between November 1998 and April 1999. Complete floor and duct plans for the house are shown in Appendix A.

The home was built in 1928, and includes 2,216 square feet of living space on two floors. Heat is provided by a naturally-drafted natural gas furnace installed in 1979. The supply ducts in the basement were also installed in 1979 and generally conform to ACCA Manual D design recommendations. The return ducts were holdovers from the original gravity warm-air system, and were modified before work began to make the return system more similar to a modern network with panned return ducts. Approximately 80 percent of the supply duct surface area and 97 percent of the return duct surface area is in the basement.

Plate 1. View of the test house from the Southeast.

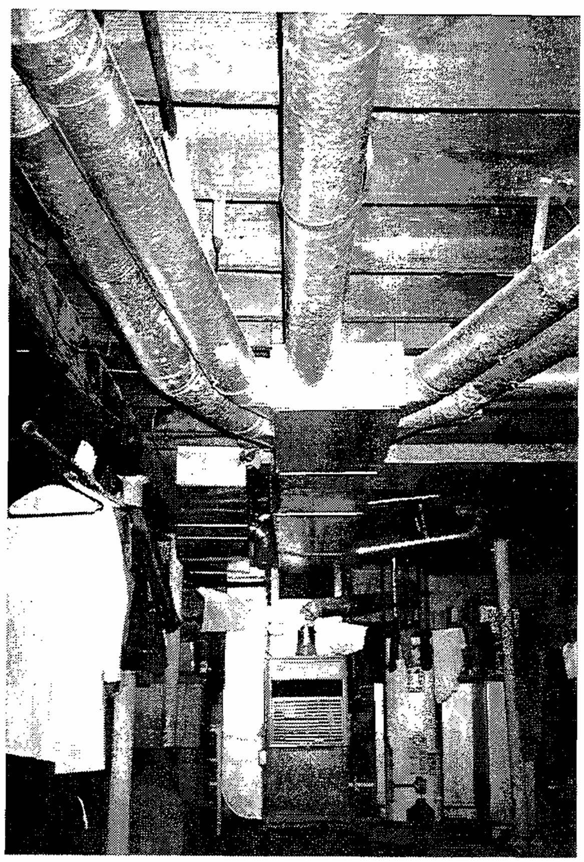

Plate 2. View of the distribution system from the West end of the basement.

The house normally runs with 12 supply registers; however, three of these were sealed for the duration of work to accommodate the capabilities of the coheating system. This left a single supply register in each of the three second-floor bedrooms, and six supply registers distributed among five first-floor rooms. The three sealed registers were located in the two bathrooms and the entrance foyer. Three return registers are present, and all are on the first floor. The existing thermostat (Hunter Set 'n Save) was left in place and controlled furnace cycling throughout the project.

Design Conditions for Syracuse: 2 °F (-16.7 °C) Heating DB - 99%;
85 °F (29.4 °C) Cooling DB - 1%;
71 °F (21.7 °C) Cooling MWB - 1%;

Standard 152P, version 98/1, was applied to each of the five duct configurations for heating. Whenever possible, diagnostic inputs were provided for 152P rather than default inputs. The required methods and accuracies for all diagnostic inputs were observed. The Standard 152P calculations for the five duct configurations are shown in Appendix D.

Three versions of the house pressure test (HPT) were conducted for each duct configuration; the methods used are explained in Appendix C.

## 2.1 Monitored Data

Three 8-channel data recorders (Simplified EZ-8), as well as a separate 13-channel data recorder (Synertech MPR-1) were installed at the house for the duration of the project to collect the various required monitored data at one-minute intervals. Temperature sensors (Simplified TP-100), anemometers (MetOne Instruments), and furnace relays (ECG) provided signals to the recorders. The temperature sensors were calibrated before the project according to the procedure in Appendix C.

Monitored data records were downloaded remotely via modem connection every second day during a monitoring period. Records were entered into the computer program used to develop the energy consumption and distribution efficiency functions intended to represent performance of a particular duct system configuration. This analysis included rejection of data records obtained during the daytime, during windy conditions, or during warmer weather, as well as other data range checking.

### 2.1.1 Benchmark Values

Two types of benchmark values were compared to 152P results:

1. Benchmark values for **relative differences** in design and seasonal heating distribution efficiency, between two different duct configurations; and
2. Benchmark values for **absolute** design and seasonal heating distribution efficiency, for each individual duct configuration.

Only heating operation was analyzed throughout this work; no cooling data was collected. Uncertainties for all benchmarks were calculated using the approach in Appendix B.

The idea with either type of benchmark was to monitor enough heating cycles to develop two different linear equations for each of the five duct configurations. For each configuration, these two equations described energy consumption rate and distribution efficiency (both y-variables), at different values of inside-outside temperature difference ($\Delta t$, x-variable). For a relative difference benchmark, the y-variable was the energy consumption rate, and consisted of the gas energy delivered to the supply plenum plus the furnace fan electrical energy, per hour. For an absolute value benchmark, the y-variable was distribution efficiency. Forty cycles were considered a minimum for strongly defining either function, and the eventual smallest group of cycles that was utilized numbered 60.

In order to develop these two equations for a given duct configuration, data was gathered during individual heating cycles. The term "cycle" here refers to the time from burner-on to burner-on. A cycle therefore included a short initial period during which the burner was on but the fan was off, a second period during which the burner and fan were both on, a third period during which the burner was off but the fan was still on, and a fourth period during which the burner and the fan were both off. Total cycle time generally varied between 30 minutes and 90 minutes, depending on the outside temperature.

Energy consumption for each cycle was expressed in Btu/hour, and was the ratio of gas Btus delivered to the supply plenum over the cycle, plus the electrical Btus delivered to the furnace fan over the cycle, to the length of the cycle in hours.

Distribution efficiency for each cycle was expressed as a decimal less than 1.0, and was the ratio of the energy that would have been used by electric coheating to maintain the cycle's average inside-outside $\Delta t$, over the length of the cycle, to the actual energy consumption for the cycle.

All analyzed cycles were collected under calm wind conditions, in order to eliminate the effect of differing wind infiltration loads from cycle to cycle. A cycle was considered calm when the average wind speed over the length of the cycle was less than 1.5 miles per hour. On-site anemometers distinguished calm cycles from windy cycles. In addition, all analyzed cycles were gathered between 7 PM and 7 AM to eliminate differing solar gains. As a result, Δt was taken to be the only environmental variable affecting load, and indicated stack effect infiltration load as well as conductive load.

Figure 1 portrays two groups of cycles from the test house, with each group reflecting a different duct configuration. Linear regression for each group provided the values needed to form an energy consumption function for the group. Energy consumption values were then calculated for x-values of $\Delta t_{design}$ and $\Delta t_{seasonal}$, and represented the expected "pre-benchmark" energy consumption rates under design and seasonal conditions, respectively. The two values for $\Delta t_{design}$ or $\Delta t_{seasonal}$ were then employed together to form a benchmark value for the **relative difference** in design or seasonal distribution efficiency, respectively, between the two configurations.

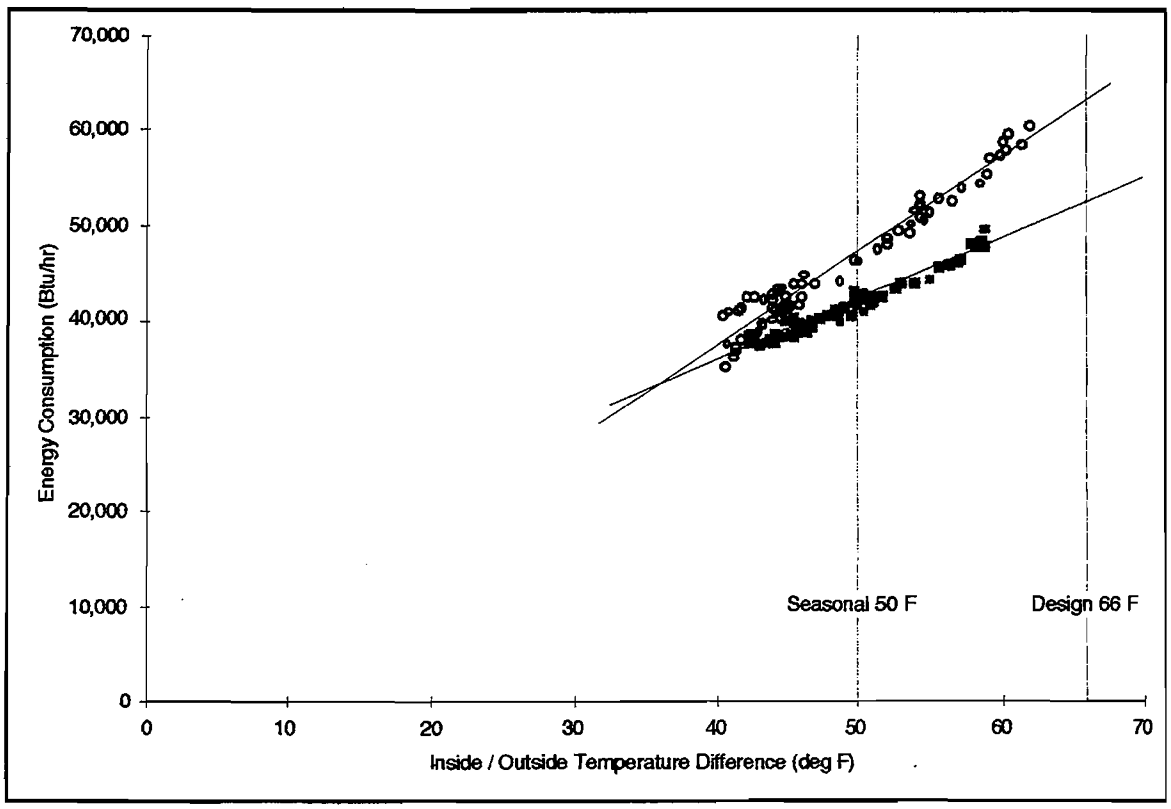


Figure 1. Two Energy Consumption Functions

For either design or seasonal conditions, two consumption values representing two different duct configurations are compared with 152P-estimated distribution efficiencies for the two configurations, according to a model of the following form:

$$\frac{E_1}{E_2} = \frac{\eta_2}{\eta_1} \tag{1}$$

where $E_1$ = energy consumption rate at design or seasonal conditions for duct configuration 1, Btu/hour;

$E_2$ = energy consumption rate at design or seasonal conditions for duct configuration 2, Btu/hour;

$E_1/E_2$ = the benchmark **relative difference** in distribution efficiency between the two duct configurations;

$\eta_1$ = Standard 152P design or seasonal distribution efficiency for duct configuration 1; and

$\eta_2$ = Standard 152P design or seasonal distribution efficiency for duct configuration 2.

Benchmark values for **absolute** design and seasonal heating distribution efficiency for each duct configuration resulted from the same monitoring of calm night cycles during normal operation, and from a separate electric coheating test (Section 2.2) that described the energy consumption required to maintain different values of $\Delta t$ at a distribution efficiency of one.

Each cycle's monitored data was combined with the coheating data to give distribution efficiency for that cycle, according to:

$$\eta_{dist,\,cycle} = \frac{E_{coheat} \times T_{cycle} \times \Delta t_{avg,cycle}}{E_{cycle} \times e_{furn,ss}} \tag{2}$$

where $\eta_{dist,\,cycle}$ = the distribution efficiency for the individual heating cycle;

$T_{cycle}$ = the length of the cycle in hours;

$\Delta t_{avg,cycle}$ = the monitored average indoor-outdoor temperature difference during the cycle, deg F;

$E_{coheat}$ = the energy consumption rate of the living space at $\Delta t_{avg,cycle}$, measured during the electric coheating test, Btu/hr· deg F;

$E_{cycle}$ = the total monitored energy consumption during the cycle, Btu; and

$e_{furn, ss}$ = the steady state furnace efficiency for the particular duct system configuration, measured during separate combustion efficiency tests.

During both normal heating and coheating periods, miscellaneous energy gains within the living space were limited to the computer and peripheral interface box that provided monitoring of room temperatures and control of the coheating system. Since these components were powered up 24 hours per day, throughout the entire project (88 watts measured), there is no adjustment for internal gains in Eq. 2.

Figure 2 portrays a heating distribution efficiency function formed from a group of cycles at the test house, illustrating a particular duct configuration. This function gave benchmark values for the **absolute** seasonal and design distribution efficiencies of the configuration.

Similarly to the process for energy consumption, each benchmark value was determined by conducting linear regression for the data set. Distribution efficiency values were then calculated for x-values of $\Delta t_{design}$ and $\Delta t_{seasonal}$ and represented efficiency under design and seasonal conditions, respectively.

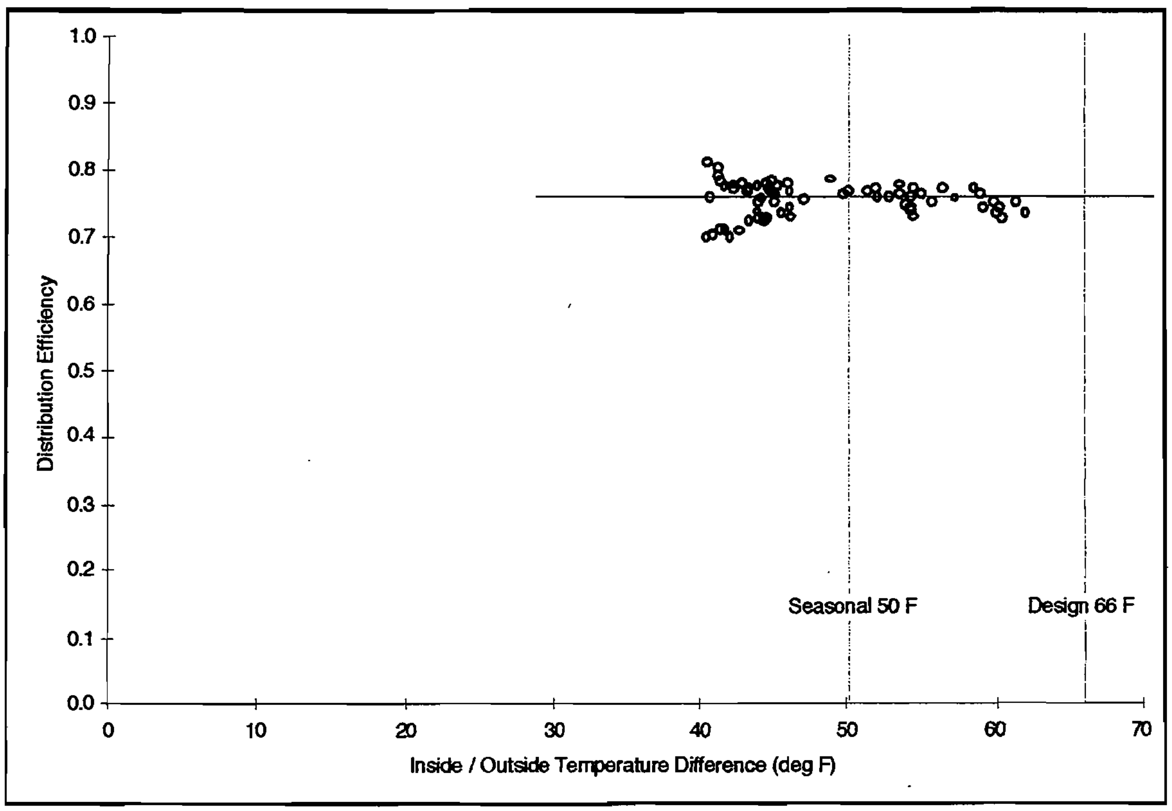


Figure 2. A Distribution Efficiency Function

### 2.1.2 Monitoring Energy

For all five duct configurations, burner and fan run-time were monitored during normal operation. These monitored run-times were combined with diagnostic measurements to give actual energy consumption rates.

For any time period, energy consumption was defined as the sum of the gas burner energy delivered to the supply plenum and the electric furnace fan energy.

Gas energy delivered to the supply plenum per minute was a product of the number of seconds of burner run-time for each one-minute monitoring interval, the measured gas flow rate to the burner, the energy content of the gas (which was shown on the monthly energy bills from the utility, and which varied less than 0.01 percent from month to month), and the steady state furnace efficiency.

Gas flow rate to the burner was measured using the house gas meter, which was a recently-calibrated meter installed by the utility (Niagara Mohawk) as work began. For each measurement, the thermostat was turned up to provide a continuous burn, and a meter reading was taken after about 10 minutes of firing. The starting reading was subtracted from the ending reading to give total gas volume during the test. The stopwatch reading at the ending meter reading was divided into total gas volume to yield flow rate.

This measurement of gas flow rate was conducted several times over the course of the project to verify consistency; each measurement was found to deviate less than one percent from the mean, which was subsequently used for all five configurations. These measurements are shown in Appendix C, along with the other measurements discussed immediately below.

Steady state furnace efficiency was measured four times during each duct configuration monitoring period, using two different combustion analyzers (Lynn 3500B, Bacharach Fyrite). The four readings were averaged to give a single measurement for the particular period. All readings over the entire project were between 80 and 84 percent.

Electrical energy consumed by the furnace fan was a product of the amperage required by the fan, measured with a clamp-on ammeter (Radio Shack 22-161) five times over the course of the project, an assumed power factor of 0.75, and the number of seconds of fan run-time for each one-minute interval. Again the multiple readings were all very close to the mean, within four percent, and the mean was used for all configurations.

### 2.1.3 Monitoring Temperatures and Δt

The following temperatures were monitored throughout the project, as one-minute averages:

1. Air temperature in each room in the conditioned space with a functioning supply register, four feet above the floor;
2. Air temperature at the thermostat, four feet above the floor;
3. Air temperature outside, four feet above grade;
4. Air temperature at two locations in the basement, two feet below the ceiling; and
5. Ground temperature at two locations outside, two feet below grade.

The locations of these sensors are shown in Appendix A. Two sensors were used at each location in 2, 3, 4, and 5 above, in order to provide redundancy and reveal individual sensor drift if it occurred. In fact two ground temperature sensors failed completely early in the project, leaving only one functioning sensor at each ground location after December.

The temperature sensors in individual rooms and at the thermostat (1 and 2 above) were used to indicate the adequacy of the alignment of coheating temperature patterns, room to room, with those observed during normal operation. Each sensor was placed near an exterior wall, but at least three feet in from the wall, in order to measure the temperature of relatively quiet air whose motion was principally controlled by natural thermal stratification in the room, even when a supply register or coheater was operating. This avoided the sharp temperature and flow gradients present around the supply registers and coheaters.

Although temperatures were monitored in each room, and in fact varied from room to room, a single "whole-house" inside temperature was needed for combination with outside temperature (3 above) in determining Δt. The temperature sensor at the thermostat (2 above) provided this inside temperature.

The temperature sensors in the basement (4 above) were used to determine when the basement had reached equilibrium during switches between normal operation and coheating, and to indicate the effect of the duct treatments on basement temperature.

Earth temperatures (5 above) were measured to detect differences in basement heating load as the winter season progressed. These temperatures are shown in Appendix C, and reveal small differences in earth temperature between the configurations.

### 2.1.4 Other Monitoring Variables

The following procedures were used to control or account for variables that could otherwise affect the accuracy of the energy consumption and distribution efficiency functions.

Despite the restriction of usable data to nighttime hours, all windows were blocked with a standard white interior shade 24 hours a day in order to limit interior heating during sunny days. In addition, above-grade sections of the masonry foundation walls on the south and west sides of the house, and the earth immediately adjacent to these walls, were shielded from sunlight by a temporary white fabric shield erected one foot away from the walls.

Lights were turned off throughout the project, and the refrigerator was unplugged. The hot water heater in the basement was allowed to run on the lowest setting, and was monitored. Its observed firing rate of 10 minutes every 50 to 60 hours was determined to be insufficient to merit incorporation into the data processing.

All interior doors except the basement door were open all the time, and the furnace filter was checked and cleaned if necessary at least every 14 days.

## 2.2 Coheating

An automated 6-day electric coheating test was conducted midway through duct configuration 1, in order to measure the energy consumption rates required to maintain different values of $\Delta t$ at a distribution efficiency equal to one. These data were necessary for calculating absolute distribution efficiency values for individual cycles. The coheating data were **not** used in computing relative differences in distribution efficiency between two duct configurations.

The coheating system (Synertech MPR-1) maintained each room's temperature steadily over time. Every 15 seconds the measured room temperature was compared to the pre-entered average room temperature observed during normal operation in configuration 1. If the measured temperature was less than the normal temperature, the room's heater ran for 15 seconds until the next temperature comparison. In fact there were two patterns of room temperatures that were used, with each reflecting a different range of $\Delta t$.

The coheaters heated the living space only, and data were collected only after the furnace had been turned off for enough time to let the basement cool and become somewhat more dependent on outside temperature (about 2 days). The coheaters were activated as the furnace was turned off, however, in order to keep the living space temperatures steady as the basement cooled. After the basement temperature stabilized in this coheat mode, energy consumption data was collected. This "cold basement" method properly included the thermal regain of duct losses from the basement to the living space in calculations of distribution efficiency.

As with the monitoring periods, all coheating data was collected between 7 PM and 7 AM, at wind speeds of less than 1.5 mph.

The following sequence of events was used in initially setting up the coheaters:

A. All supply and return registers were sealed;
B. Each coheater was placed immediately in front of or on top of the supply register it temporarily replaced, and oriented to match the direction of throw from the supply register;
C. Each coheater's air flow magnitude was adjusted to match the supply register flow magnitude as closely as possible; and
D. The equivalence of these air flow dynamics was tested using theatrical fog injected into the supply ducts and coheater intakes.

Electrical energy supplied to the living space during the coheating test was measured using a high-quality current transformer, with a manufacturer's stated accuracy of one percent, installed on the main power line that fed the heaters. The energy used to run the small fans in the heaters was included as well. This method of measurement was checked against the house electrical meter's measurement, both with all heaters running and with half of the heaters running. It was found that the house meter reading was three percent higher at 54 amps and one percent higher at 30 amps. Appendix C shows a plot of the current draw for the valid coheating data records; the current transducer's measurement was allowed to stand in all cases.

Further, during the coheating test, two different single-zone carbon dioxide ($CO_2$) tracer decay tests, with concentration analyzers (Engelhard Telaire 1050) at three locations in the living space, were conducted to test the appropriateness of the 1.5 mph wind speed threshold. As shown in Appendix C, these two tests indicated that changes in infiltration due to differences in wind speed below 2.5 mph were very small or undetectable.

# 3. RESULTS

Table 1 summarizes the diagnostic test results from the project. Key project events are then summarized in chronological sequence, and the final monitored data sets are shown. Comparisons of the benchmark values with the Standard 152P predictions and discussion of these comparisons are followed by an examination of the various duct leakage test results to conclude the section.

Table 1. Primary Diagnostic Results

| | Duct Configuration | | | | |
|---|---|---|---|---|---|
| | 1<br>Supply and Return Sealed | 2<br>Supply Leakage Only | 3<br>Supply Leakage and Return Leakage | 4<br>Return Leakage Only | 5<br>Supply and Return Sealed; Supply Insulated |
| Avg. Supply Pressure Pan (Pa) | 21.2 | 15.0 | 14.1 | 22.2 | 23.8 |
| Return Plenum Pressure (Pa) | -7.6 | -7.6 | -7.5 | -6.5 | -7.4 |
| Supply Duct Leakage (CFM) | 138 | 303 | 315 | 169 | 147 |
| Return Duct Leakage (CFM) | 77 | n/a | 382 | 329 | 87 |
| Furnace Fan Flow (CFM) | 745 | 721 | 789 | 727 | 736 |
| Design Distribution Efficiency Standard 152P | 0.69 | 0.58 | 0.63 | 0.70 | 0.78 |
| Seasonal Distribution Efficiency Standard 152P | 0.67 | 0.57 | 0.60 | 0.67 | 0.75 |

## *3.1 CONFIGURATION 1 AND COHEATING WORK*

Configuration 1 was created by sealing all of the supply and return ducts in the basement with a combination of mastic and foil tape, before configuration 1 testing or monitoring began. This included the sealing of building bypasses in the vicinity of ducts. A fog generator and duct pressurization fan were used to track sealing progress and to identify remaining leaks at various stages.

The sealing was completed on November 15, 1998, with the supply leakage flow still higher than expected (138 CFM), but with no visible evidence of further leaks in accessible ducts. Twenty percent of the remaining measured supply leakage flow tested as outside leakage rather than basement leakage during an outside-only leakage test, perhaps indicating leaks in the second level floor framing space. This space was observed to be open to one ventilated crawlspace adjoining an upstairs bedroom.

If the supply leakage measurement and calculation were accurate, the remaining 80 percent presumably reflected leakage in first floor partition walls that somehow resolved as basement or outside leakage in inobvious ways.

After 18 additional days spent testing and calibrating sensors, conducting envelope air leakage tests, measuring furnace fuel delivery rate and steady state efficiency (SSE), and setting up the electric coheating system, monitoring of configuration 1 performance began on December 4, 1998.

On December 18, the furnace was turned off, all supply and return registers were sealed, and the coheating test began. The coheating test eventually provided 18 hours of valid data which were used to describe the energy consumption rate of the living space as a function of $\Delta t$, at a heating distribution efficiency of one. This relationship was incorporated into all calculated benchmark distribution efficiency values.

On December 24 the coheaters were turned off and the furnace was re-activated. Additional configuration 1 normal operation data were collected from December 31 to January 14, 1999. On January 10 the final diagnostic tests were conducted to complete the description of configuration 1.

Figure 3 shows the coheating data used to convert each cycle's monitored energy consumption data to distribution efficiency data. The coheating relationship shown in Figure 3 was applied to energy consumption data from all five duct configurations in order to calculate distribution efficiencies.

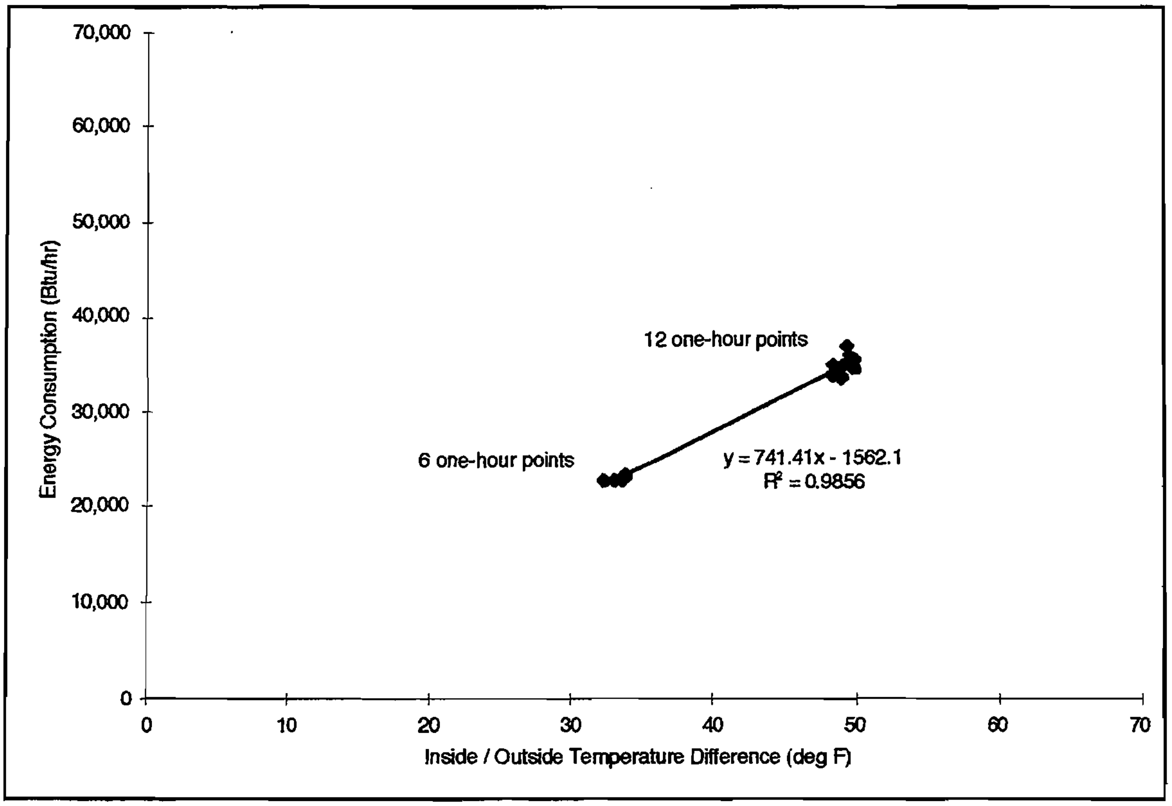


Figure 3. Energy Consumption; Coheating Test

Figure 4 shows the energy consumption rates associated with the normal heating cycles from configuration 1, while the distribution efficiency data for configuration 1 are shown in Figure 5. The design and seasonal Δt values for Syracuse, NY of 66 deg F and 50 deg F, respectively, are marked on these figures and the following similar figures; these are the values of Δt at which distribution efficiency is estimated by Standard 152P.

The sets of normal heating cycles shown in the following figures may be subsets of all of an individual configuration's usable data, in order to obtain the smallest uncertainty in the benchmark values. Whole data sets were pared to more accurate subsets by increasing the minimum Δt required for inclusion. Further, the most accurate energy consumption data set may be different from the most accurate distribution efficiency data set.

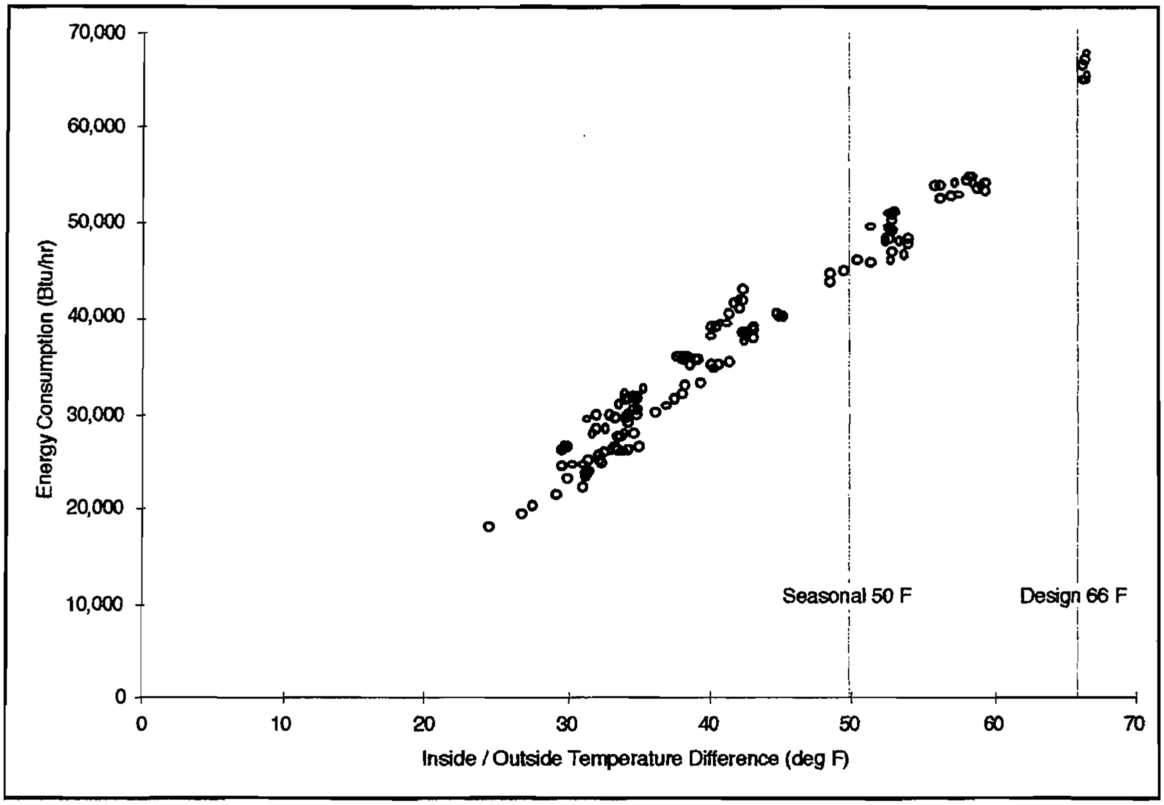


Figure 4. Energy Consumption; Duct Configuration 1, 138 Normal Cycles

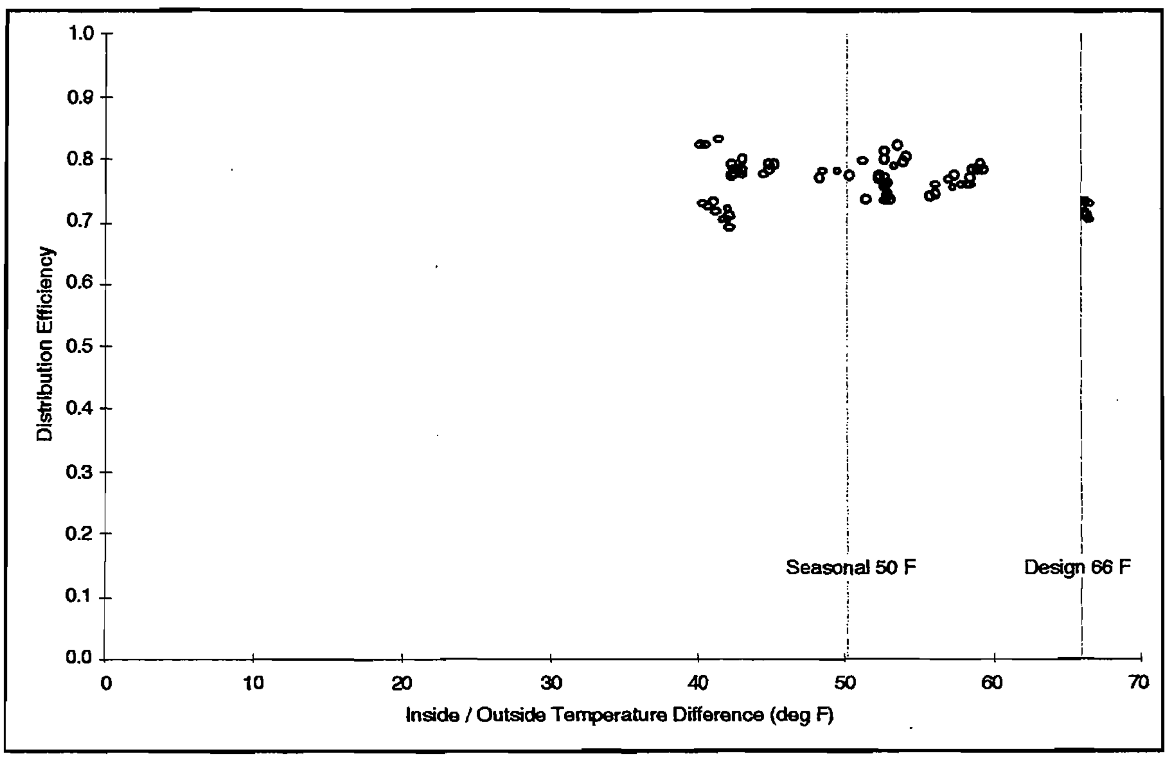


Figure 5. Distribution Efficiency; Duct Configuration 1, 68 Normal Cycles

### 3.2 CONFIGURATION 2 WORK

Following configuration 1, a new natural gas meter was installed, fresh from the utility's meter shop. This was done to increase our confidence in our gas delivery rate measurement. In fact a single measurement taken using the new meter was within 0.02 percent of our measurement using the original meter.

Configuration 2 was initiated on January 16 by adding supply duct leakage. A power sheet metal nipper was used to create 1/4" wide slots throughout the supply duct system. For round ducts each slot was 12" to 24" long and parallel to the duct run, while for the rectangular plenum each slot was 6" long and perpendicular to the run. Two 16" long slots were added to the supply plenum as well. Total added physical supply leakage area was approximately 100 square inches.

The configuration 2 diagnostic tests were conducted on January 16 and January 17. Configuration 2 normal operation data were collected from January 18 to February 1. Figure 6 shows energy consumption for configuration 2, while Figure 7 shows the distribution efficiency data.

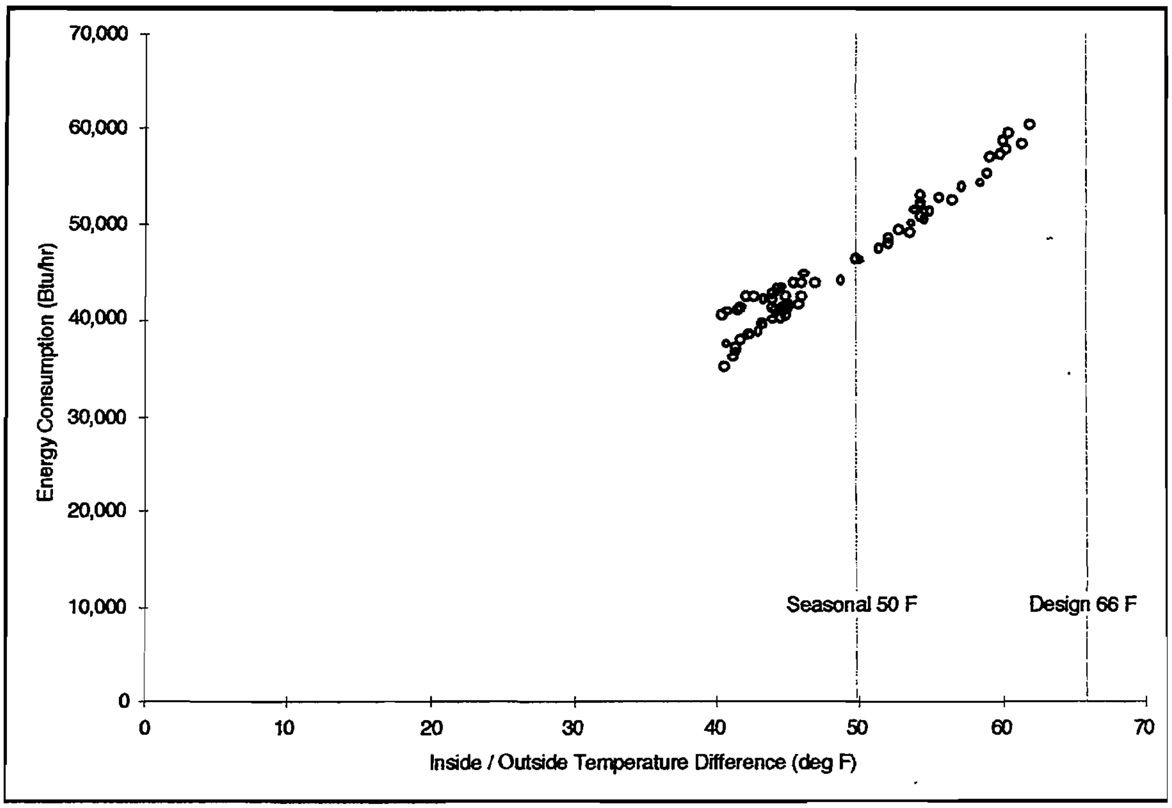


Figure 6. Energy Consumption; Duct Configuration 2, 73 Normal Cycles

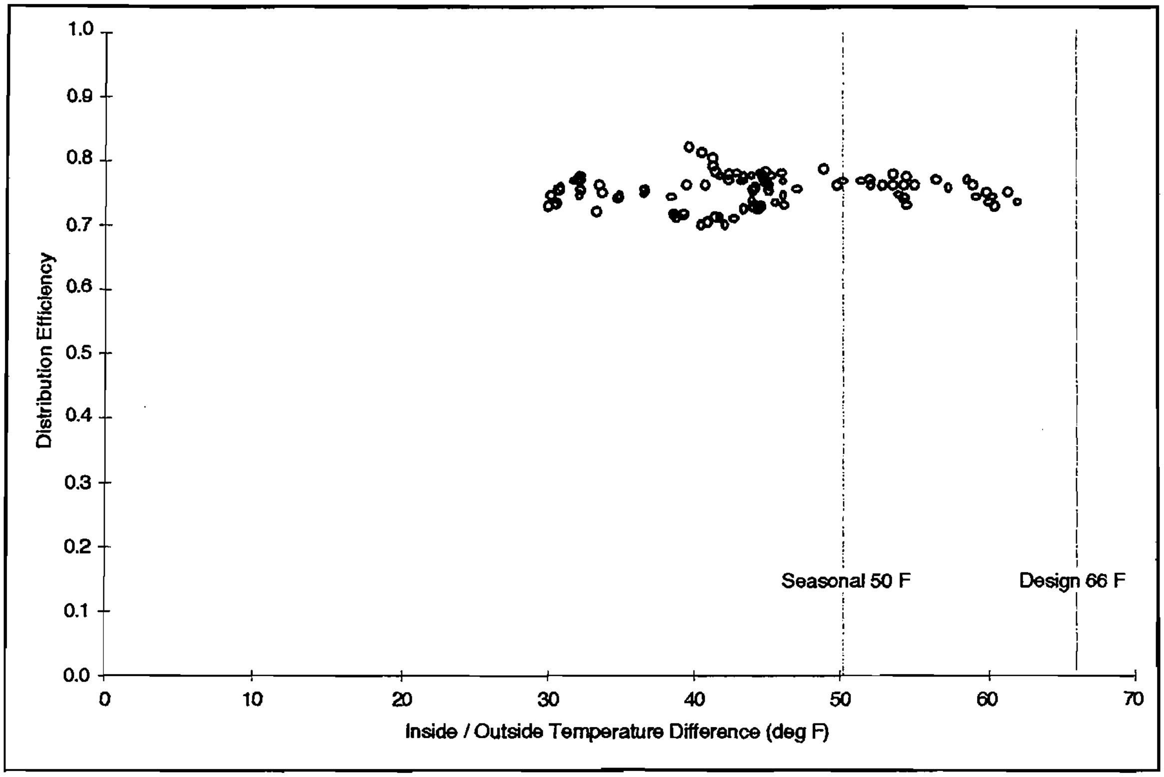


Figure 7. Distribution Efficiency; Duct Configuration 2, 101 Normal Cycles

### 3.3 CONFIGURATION 3 WORK

Configuration 3 was initiated on February 1 by adding return duct leakage; the nipper was used to create 1/4" to 1" wide slots in the return ducts. As with the supply leakage, the return leakage was spread out over the entire return system. Slots in panned ducts were made in the metal panning material, and were perpendicular to the direction of flow. Total added physical return leakage area was approximately 200 square inches.

Configuration 3 normal operation data were collected from February 3 to February 15. The configuration 3 diagnostic tests were conducted for the most part on February 16. Figure 8 shows energy consumption for configuration 3, while the distribution efficiency data is shown in Figure 9.

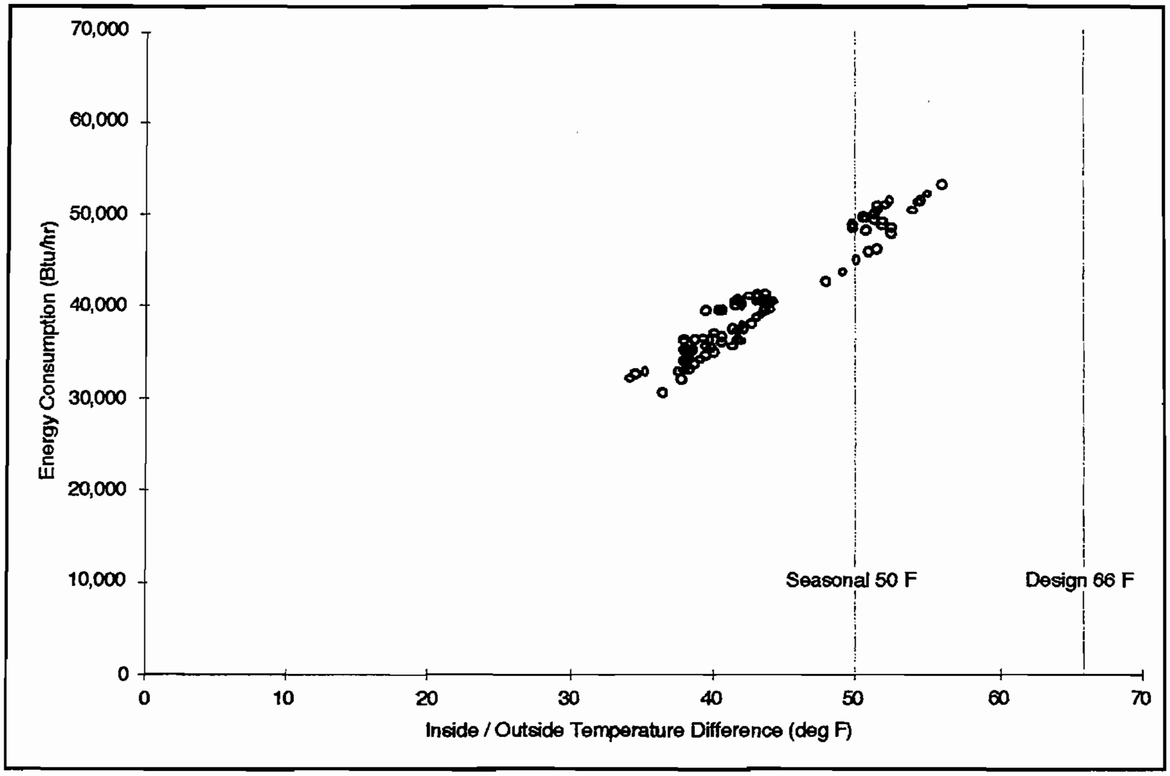


Figure 8. Energy Consumption; Duct Configuration 3, 90 Normal Cycles

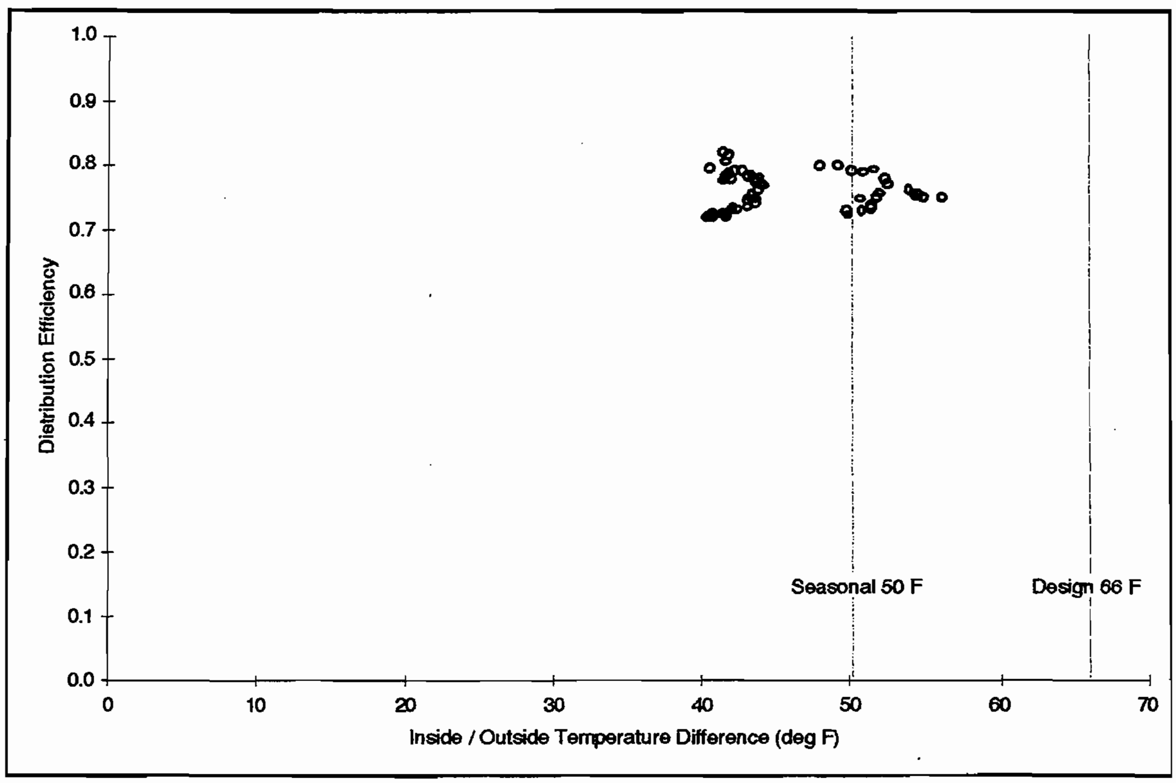


Figure 9. Distribution Efficiency; Duct Configuration 3, 60 Normal Cycles

### 3.4 CONFIGURATION 4 WORK

Configuration 4 was initiated on February 16 by sealing the previously added supply duct leakage (used to create configuration 2), using foil tape.

Configuration 4 normal operation data were collected from February 17 to March 7. The configuration 4 diagnostic tests were conducted on March 2. Figure 10 shows energy consumption for configuration 4, while the distribution efficiency data is shown in Figure 11.

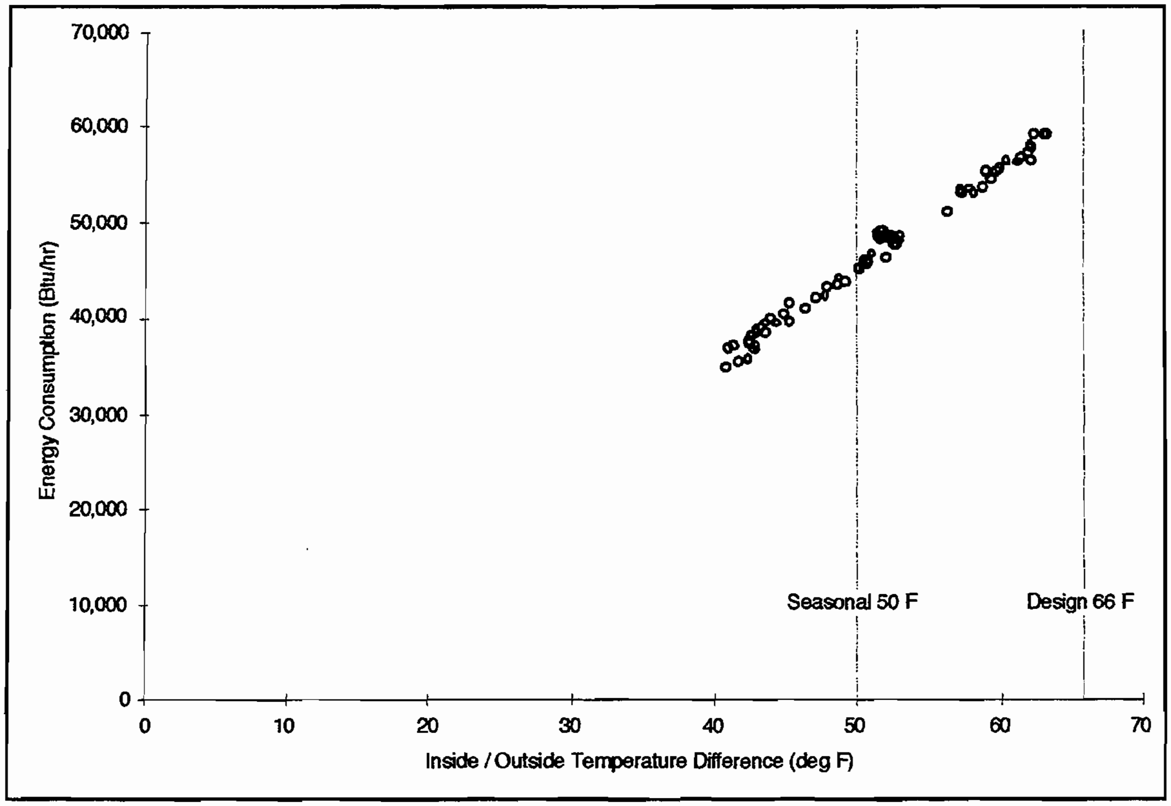


Figure 10. Energy Consumption; Duct Configuration 4, 72 Normal Cycles

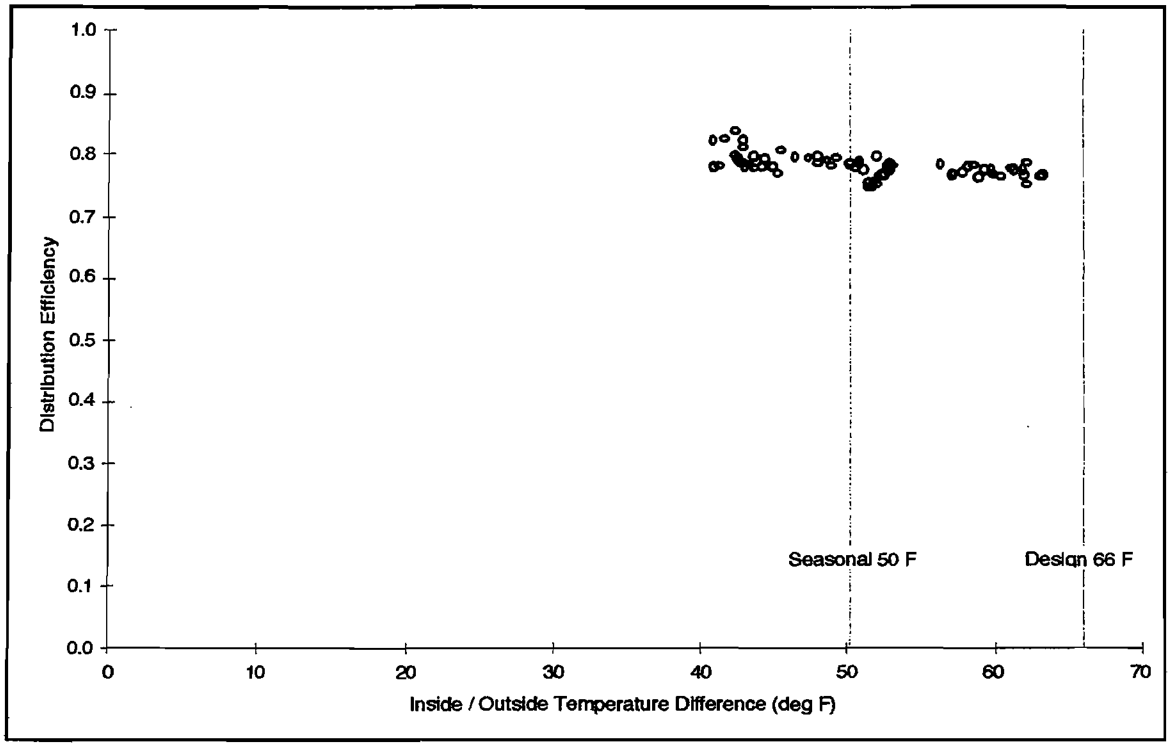


Figure 11. Distribution Efficiency; Duct Configuration 4, 72 Normal Cycles

### 3.5 CONFIGURATION 5 WORK

Configuration 5 was initiated on March 8 by sealing the previously added return duct leakage (used to create configuration 3), again using foil tape. Most of the supply ducts were insulated as well, using standard foil scrim faced low-density fiberglass ductwrap. This product has an installed R-value of 8.3. The insulation was secured using divergent-point staples, and foil tape was used to cover all seams.

The entire supply trunk was insulated, as well as most of the basement branch duct surface area. Basement supply duct termination points at ceiling boots were left uninsulated, due to the time required to fit ductwrap onto the elbows and boots. The supply plenum was left uninsulated as well, due to the presence of a close-fitting branch duct on one side, the close return plenum on a second side, and the high-temperature furnace vent on a third side. Appendix A shows the duct insulation coverage.

Configuration 5 data were collected from March 9 to March 20. The configuration 5 diagnostic tests were conducted on April 2. An unauthorized individual decreased the thermostat setpoint on March 20, unfortunately preventing inclusion of warmer-weather data. Figure 12 shows energy consumption for the heating cycles available from configuration 5, while the distribution efficiency data is shown in Figure 13.

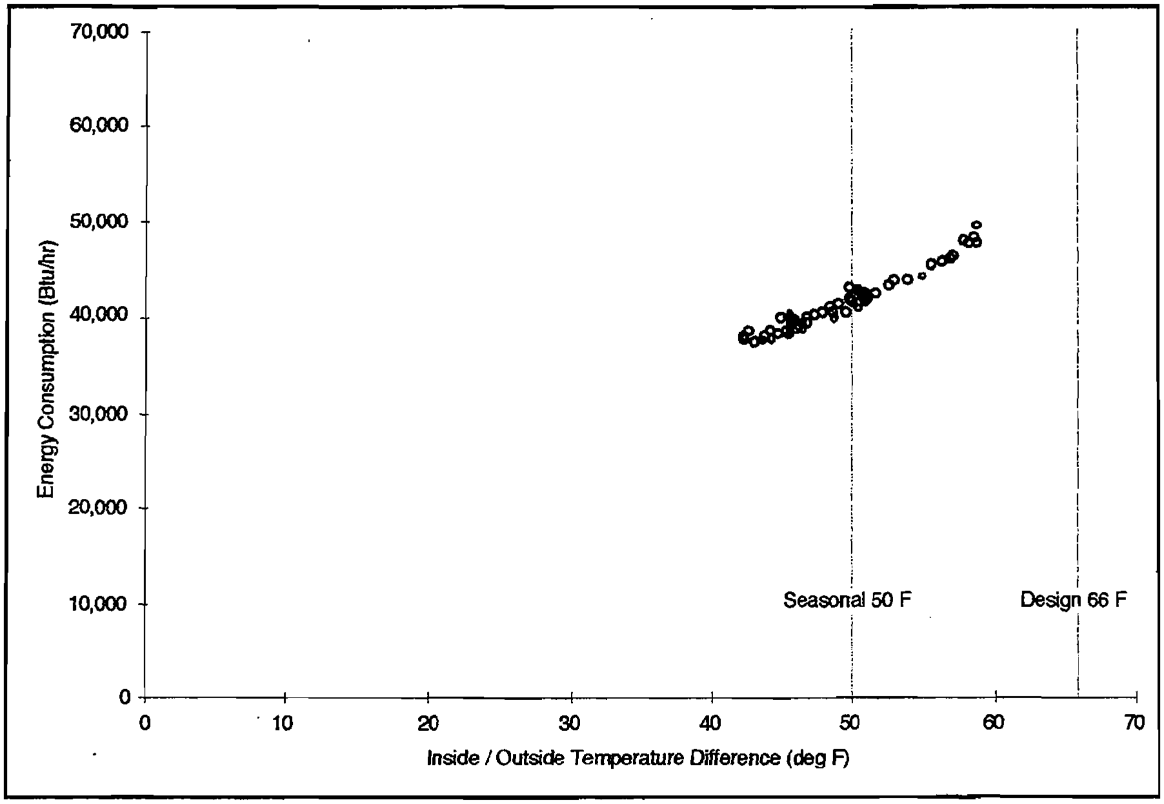


Figure 12. Energy Consumption; Duct Configuration 5, 63 Normal Cycles

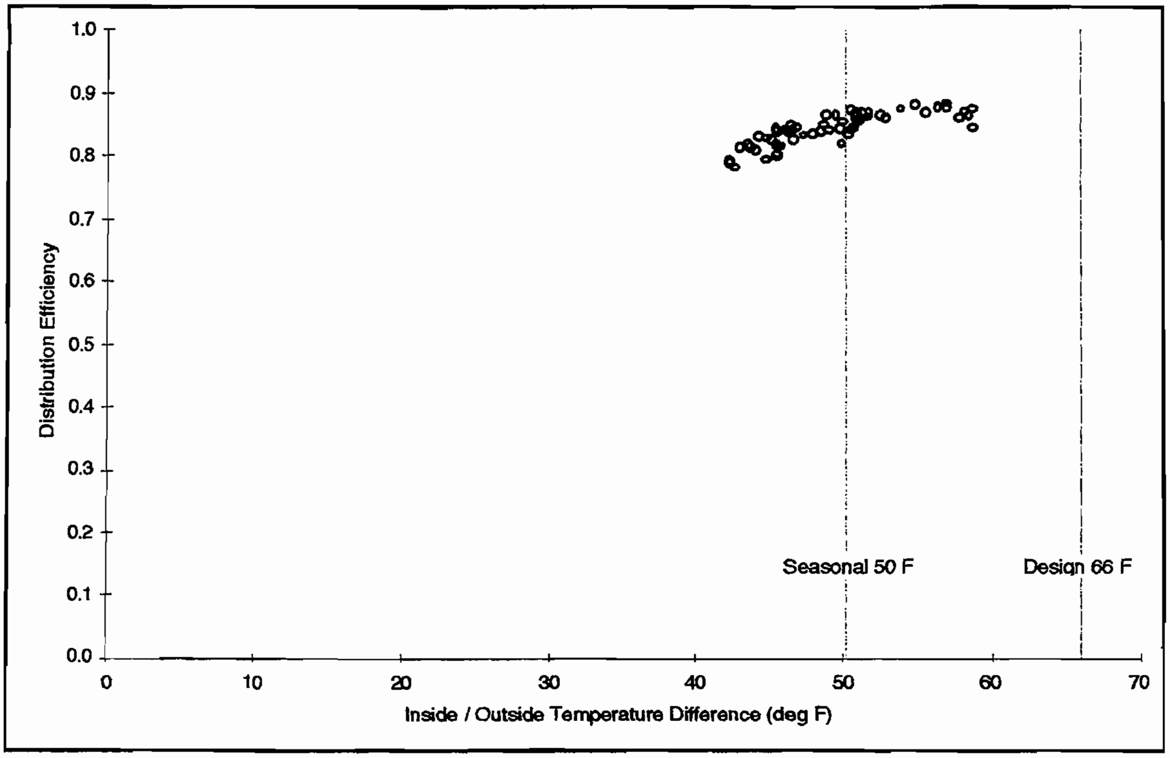


Figure 13. Distribution Efficiency; Duct Configuration 5, 63 Normal Cycles

### 3.6 COMPARISON OF BENCHMARKS WITH STANDARD 152P

Tables 2 and 4 below compare the benchmark values with the values predicted by Standard 152P. Table 3 shows the intermediate "pre-benchmark" energy consumption rates that were produced for the five configurations, which were used to generate the relative difference benchmark values in Table 4. Table 4 uses configuration 5 as the common comparator, due to the relative accuracy of its values in Tables 2 and 3 and hence the relative accuracy of any quotient it is incorporated into. All uncertainties were calculated using a 95 percent confidence level.

Table 2. Design and Seasonal Standard 152P and Absolute Benchmark Values for Distribution Efficiency

| | Duct Configuration | | | | |
|---|---|---|---|---|---|
| | 1 Supply and Return Sealed | 2 Supply Leakage Only | 3 Supply Leakage and Return Leakage | 4 Return Leakage Only | 5 Supply and Return Sealed; Supply Insulated |
| Design Distribution Efficiency Standard 152P | 0.69 | 0.58 | 0.63 | 0.70 | 0.78 |
| Design Distribution Efficiency Benchmark | 0.75 | 0.75 | 0.74 | 0.76 | 0.92 |
| Benchmark Percent Uncertainty | 9.0 | 6.7 | 8.9 | 4.0 | 3.7 |
| Seasonal Distribution Efficiency Standard 152P | 0.67 | 0.57 | 0.60 | 0.67 | 0.75 |
| Seasonal Distribution Efficiency Benchmark | 0.76 | 0.75 | 0.75 | 0.78 | 0.85 |
| Benchmark Percent Uncertainty | 8.6 | 6.5 | 7.8 | 3.8 | 3.6 |

Table 2 shows that there is substantial disagreement between the absolute benchmark values for distribution efficiency and the predictions of Standard 152P, for both design and seasonal values. While the relatively large uncertainties found for configuration 1 allows possible agreement of the two methods for design conditions, this is not the case for the nine other cells in Table 2. Further, if the uncertainties apply similarly to design and seasonal values, the discrepancies between the benchmarks and Standard 152P predictions widen for seasonal performance versus design performance, except for configuration 5.

The benchmark values in Table 2 indicate a conclusive increase in distribution efficiency if any of the first four configurations are changed to configuration 5, whereas it is unclear that switching between any of the other four configurations changes distribution efficiency.

Table 3. Design and Seasonal Pre-Benchmark Values for Energy Consumption

| | Duct Configuration | | | | |
|---|---|---|---|---|---|
| | 1<br>Supply and Return Sealed | 2<br>Supply Leakage Only | 3<br>Supply Leakage and Return Leakage | 4<br>Return Leakage Only | 5<br>Supply and Return Sealed; Supply Insulated |
| Design Energy Consumption (Btu/hr) | 63,821 | 63,155 | 64,044 | 62,037 | 52,241 |
| Percent Uncertainty | 6.3 | 4.3 | 5.3 | 2.7 | 3.0 |
| Seasonal Energy Consumption (Btu/hr) | 46,522 | 47,334 | 47,227 | 45,467 | 41,956 |
| Percent Uncertainty | 8.5 | 5.6 | 6.6 | 3.6 | 3.4 |

Table 4. Design and Seasonal Standard 152P and Benchmark Values for Relative Differences in Distribution Efficiency

| | Duct Configuration Pairings | | | |
|---|---|---|---|---|
| | Conf 5<br>Conf 1 | Conf 5<br>Conf 2 | Conf 5<br>Conf 3 | Conf 5<br>Conf 4 |
| Design Quotient Standard 152P Values (*x / 5*) | 0.885 | 0.744 | 0.808 | 0.897 |
| Design Quotient Benchmark Values (*5 / x*) | 0.819 | 0.827 | 0.816 | 0.842 |
| Benchmark Percent Uncertainty | 7.0 | 5.3 | 6.1 | 4.1 |
| Seasonal Quotient Standard 152P Values (*x / 5*) | 0.893 | 0.760 | 0.800 | 0.893 |
| Seasonal Quotient Benchmark Values (*5 / x*) | 0.902 | 0.886 | 0.888 | 0.923 |
| Benchmark Percent Uncertainty | 9.1 | 6.6 | 7.5 | 4.9 |

In Table 4, each "quotient" based on Standard 152P values is calculated by dividing configuration 5 152P distribution efficiency into configuration *x* 152P distribution efficiency, where both configurations' distribution efficiency values are obtained from Table 2. Each benchmark quotient is calculated by dividing configuration $x$ energy consumption into configuration 5 energy consumption, where both configurations' energy consumption values are obtained from Table 3. Refer to Eq. 1 in Section 2.1.1.

One possible source of the lower efficiencies indicated by Standard 152P is an overestimation of supply duct leakage in the basement. Register flow measurements during normal furnace fan operation were collected for configurations 1 and 3, and are detailed in Appendix C. For any individual configuration, the actual total supply register flow plus the actual supply duct leakage flow must be less than or equal to the measured furnace fan flow. Thus the register measurements are useful for checking the duct leakage measurement.

For configuration 1, total measured supply register flow equaled 865 CFM, while calculated supply duct leakage flow equaled 138 CFM. However, the measured furnace fan flow was only 745 CFM. A hot-wire anemometer traverse of the return plenum was in reasonably good agreement with the fan flow measurement at 712 CFM. Thus the total register flow measurement is likely an over-estimation by at least 15 percent, since it exceeds the measured fan flow, and the over-estimation is close to 30 percent if the duct leakage flow calculation is accurate. This may indicate that the calculated supply duct leakage flow is itself an over-estimation.

For configuration 3, total measured supply register flow equaled 724 CFM, while calculated supply duct leakage flow equaled 315 CFM. Again the measured furnace fan flow, at 789 CFM, was less than the sum of register flow and leakage flow, suggesting that supply duct leakage is over-estimated.

Lower supply duct leakage flow values would raise the Standard 152P values for distribution efficiency in Table 2 closer to the benchmark values.

## 3.7 DUCT LEAKAGE TEST COMPARISONS

Each of the five duct configurations were subjected to four different air leakage tests which measured supply and return leakage separately:

1. The standard fan pressurization test, which requires that a physical barrier be placed between the supply and return ducts, and that each side be pressurized separately;
2. The hybrid fan pressurization test, which requires only that the entire duct system be pressurized, without a barrier in place, and that the dominant duct leakage portion of the house pressure test (HPT) be conducted;
3. The return-blocked HPT, which does not require duct pressurization; and
4. The supply-blocked HPT, which also does not require duct pressurization.

The individual supply and return fan pressurization tests are often expected to result in the most accurate measurements of leakage flow at particular test pressures, although application of inaccurate actual duct operating pressures can still cause error in the leakage flow estimates.

Table 5 compares the results of the standard fan pressurization tests with the results of the hybrid fan pressurization tests, for the five different duct configurations. Each configuration includes three hybrid results based on three different sets of house pressure data and a single fan pressurization test.

Table 5. Standard and Hybrid Fan Pressurization Duct Leakage Test Results

| | Duct Configuration | | | | |
|---|---|---|---|---|---|
| | 1<br>Supply and Return Sealed | 2<br>Supply Leakage Only | 3<br>Supply Leakage and Return Leakage | 4<br>Return Leakage Only | 5<br>Supply and Return Sealed; Supply Insulated |
| Supply Duct Leakage Standard Test (CFM) | 138 | 303 | 315 | 169 | 147 |
| Supply Duct Leakage Hybrid Test (CFM) | 137<br>153<br>157 | 288<br>300<br>284 | 413<br>500<br>571 | 208<br>357<br>353 | 118<br>254<br>21 |
| Return Duct Leakage Standard Test (CFM) | 77 | n/a | 382 | 329 | 87 |
| Return Duct Leakage Hybrid Test (CFM) | 112<br>107<br>105 | 160<br>155<br>162 | 399<br>360<br>328 | 425<br>378<br>379 | 109<br>65<br>141 |

Table 5 shows that the hybrid fan pressurization test results are largely in reasonable agreement with the standard fan pressurization results. This is particularly encouraging in light of the high envelope flow coefficient measured for the test house, since the hybrid test does require fan-off and fan-on house pressure measurements with unblocked registers. A leaky envelope is generally thought to make it more difficult to clearly distinguish the house pressure consequence of one of these conditions from the other.

Figures 14 through 23 show the results of the blocked-return and blocked-supply house pressure tests for the five different duct configurations. The house pressure tests were repeated three times for each duct configuration, and each of the three data sets produced multiple estimates of duct leakage. Each figure includes all of the valid leakage estimates from all three house pressure tests for the given configuration, for either supply or return sides.

Summary comments on the duct leakage results are offered following Figures 14-23.

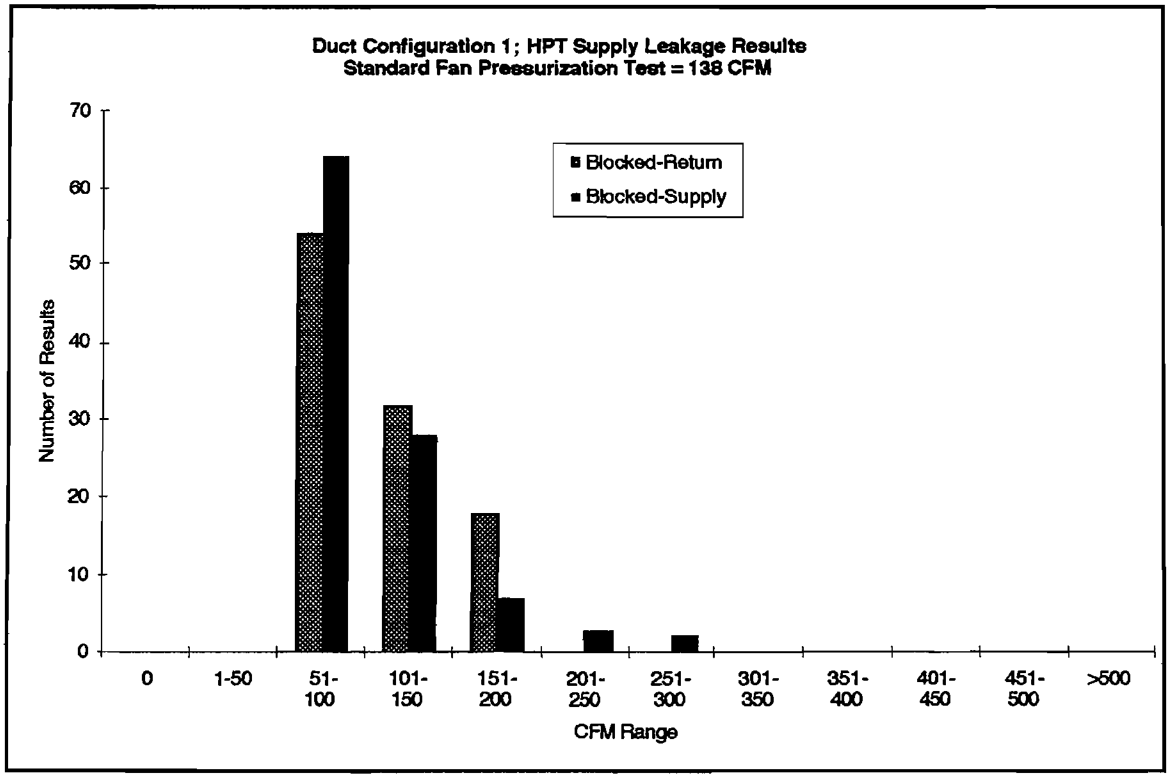


Figure 14. HPT Supply Leakage Results; Configuration 1

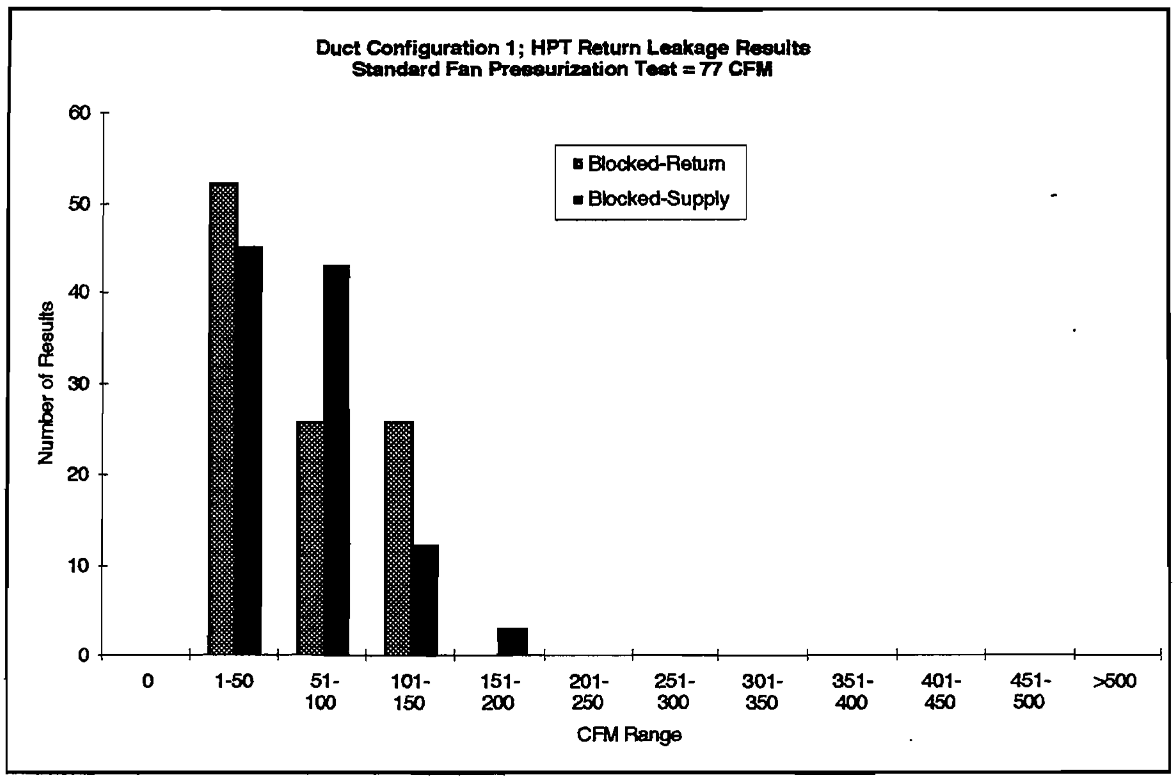


Figure 15. HPT Return Leakage Results; Configuration 1

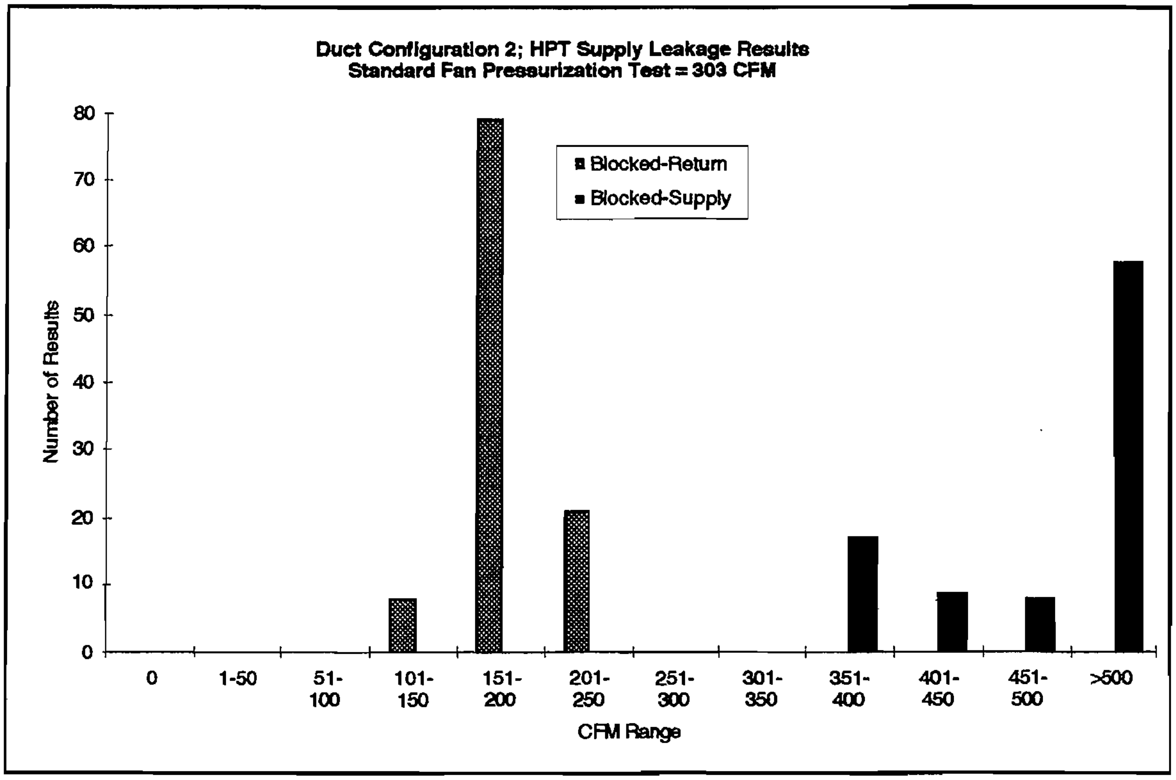


Figure 16. HPT Supply Leakage Results; Configuration 2

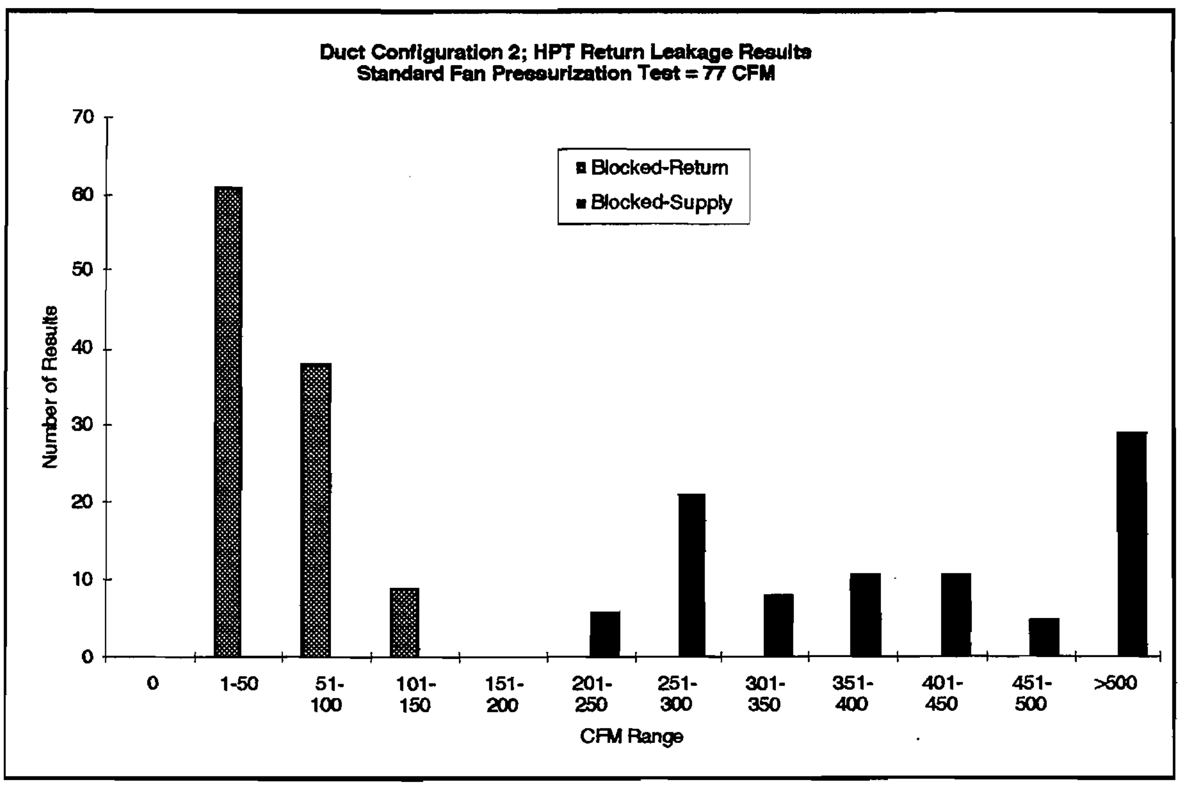


Figure 17. HPT Return Leakage Results; Configuration 2

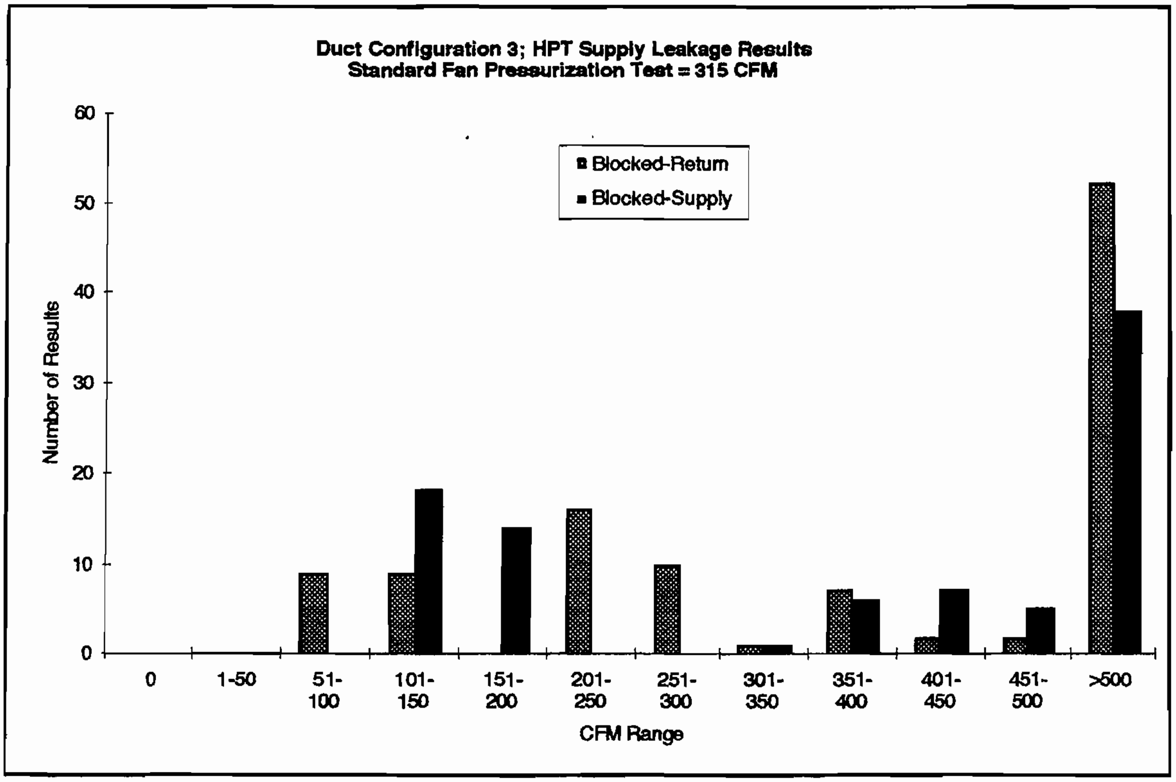


Figure 18. HPT Supply Leakage Results; Configuration 3

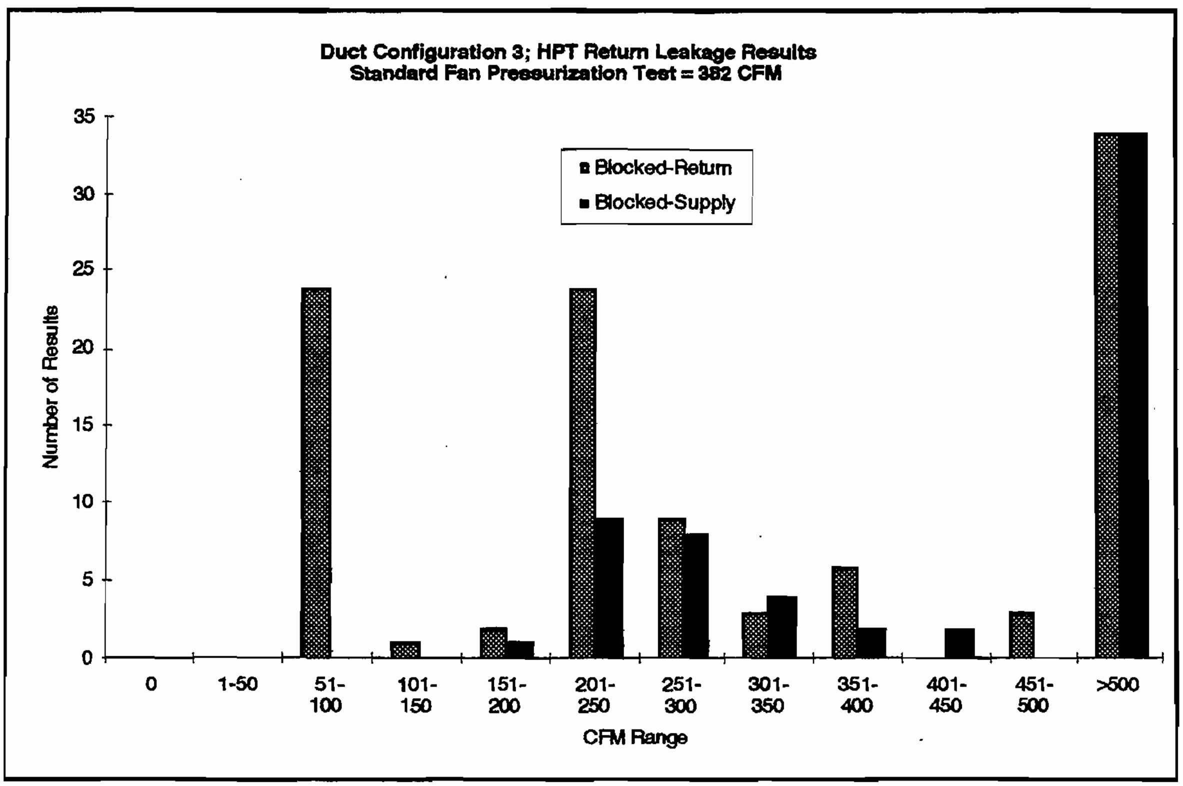


Figure 19. HPT Return Leakage Results; Configuration 3

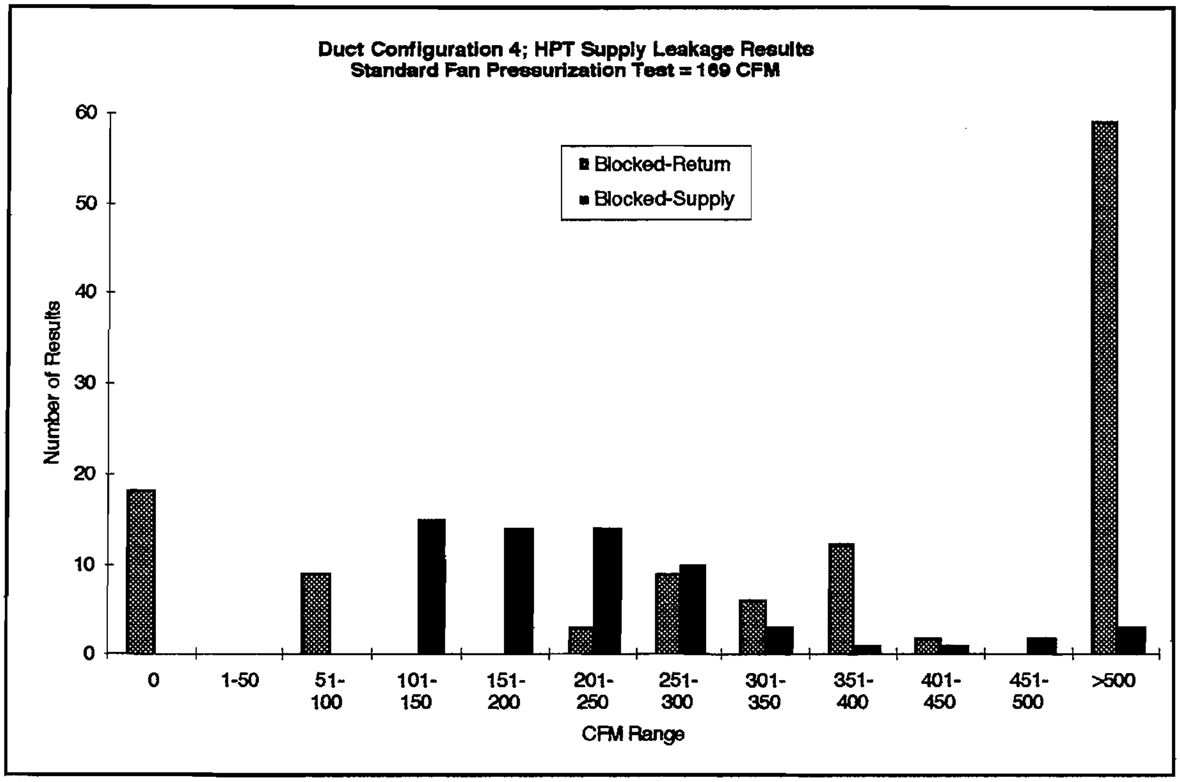


Figure 20. HPT Supply Leakage Results; Configuration 4

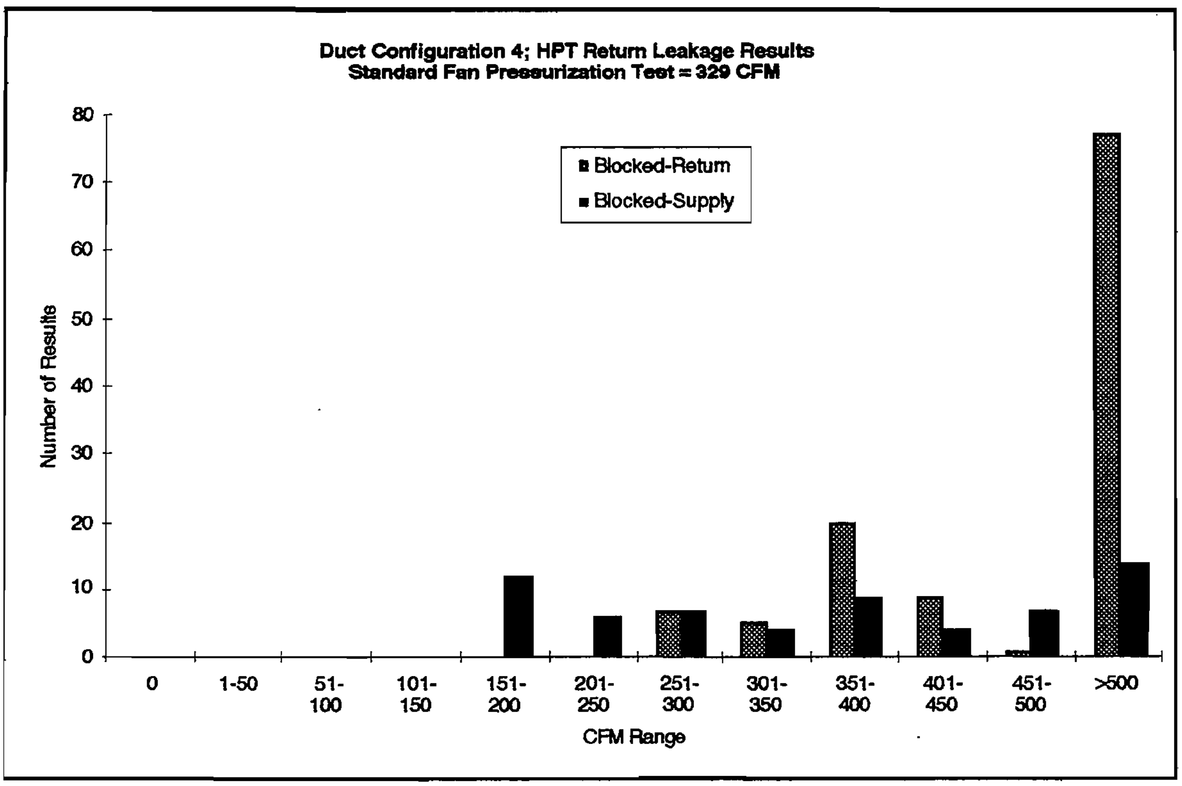


Figure 21. HPT Return Leakage Results; Configuration 4

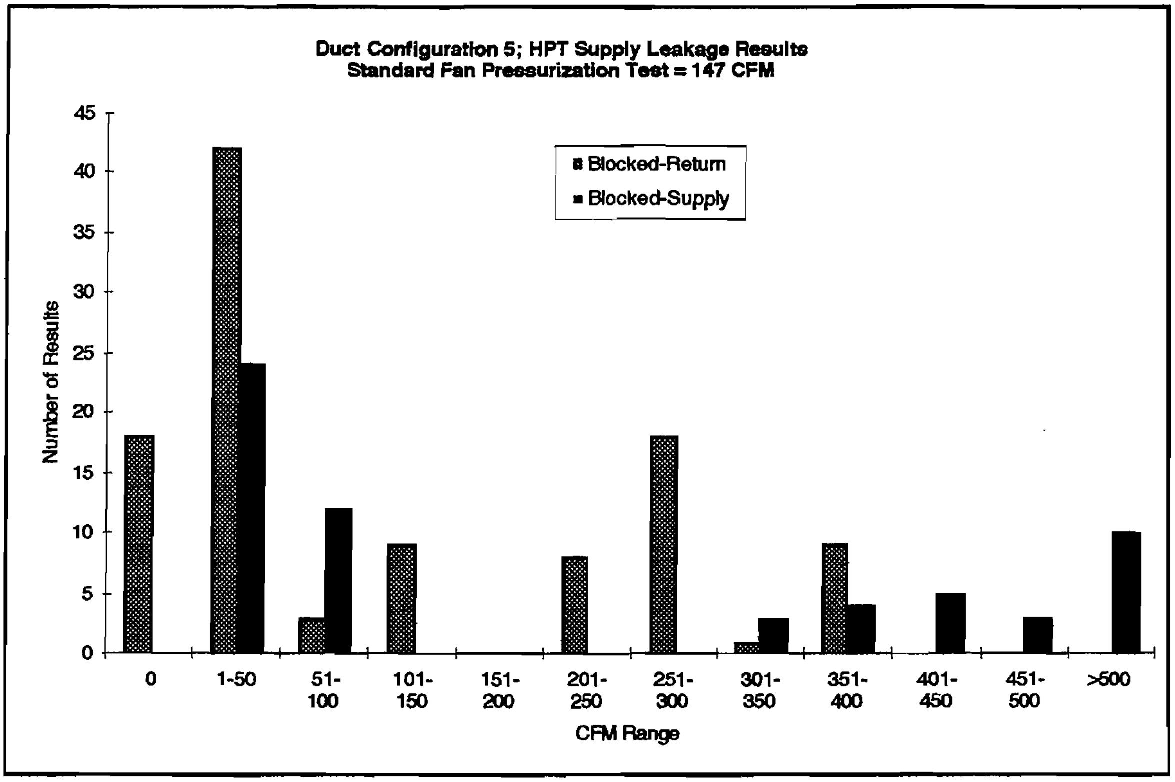


Figure 22. HPT Supply Leakage Results; Configuration 5

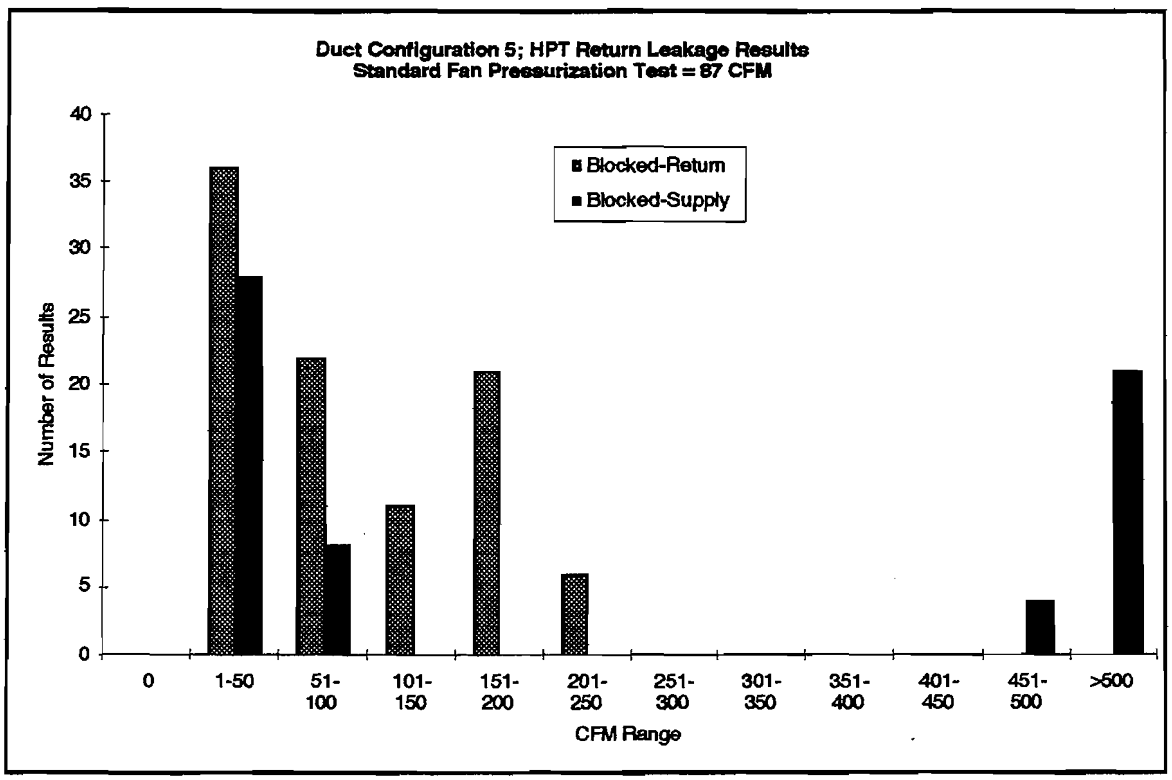


Figure 23. HPT Return Leakage Results; Configuration 5

The following comments can be made on the leakage results for the five configurations:

Configuration 1: Good agreement was obtained between the hybrid test and the standard test. The HPT results were consistent with these.

Configuration 2: Good agreement was obtained between the hybrid test and the standard test. The blocked-return HPT results were consistent with these, while the blocked-supply HPT results gave an unacceptably broad (nonrepeatable) spread of values.

Configuration 3: Good agreement was obtained between the hybrid test and the standard test. Both house pressure tests gave an unacceptably broad spread of values.

Configuration 4: Good agreement was obtained on the return side between the hybrid test and the standard test. On the supply side, the hybrid test gave significantly higher values for leakage than the standard test. Both house pressure tests gave unacceptably broad spreads of values.

Configuration 5: The hybrid test gave an unacceptably broad spread of values for leakage on both the supply and return sides, though on average the hybrid results were consistent with the standard test results. Both house pressure tests gave unacceptably broad spreads of values.

The following general conclusions can be stated concerning the duct leakage test results:

1. The house pressure tests gave unacceptably broad, nonrepeatable spreads of values in most cases. This house posed a particularly difficult problem for the house pressure test for four reasons: a) there are three return registers; b) the filter is at the furnace; c) the return duct pressure is unusually low (less than 8 Pa at the plenum); and d) the envelope leakage coefficient is high (CFM50 in the 5,000 - 6,000 range). The house pressure test is expected to work best when there is only one return register, the filter is at this register, the duct pressures are reasonably high (tens of pascals), and the envelope flow coefficient is low to moderate.
2. Given the high envelope flow coefficient, the hybrid test (which depends on house pressure measurements with unblocked registers) worked remarkably well. With a suitable criterion for how many house pressure points to take, it may be quite acceptable for diagnostic work. For maximum accuracy at the price of somewhat

greater testing time, combining the results of the hybrid and standard duct pressurization tests is probably the best approach.

# Appendix A
# House and Duct Plans

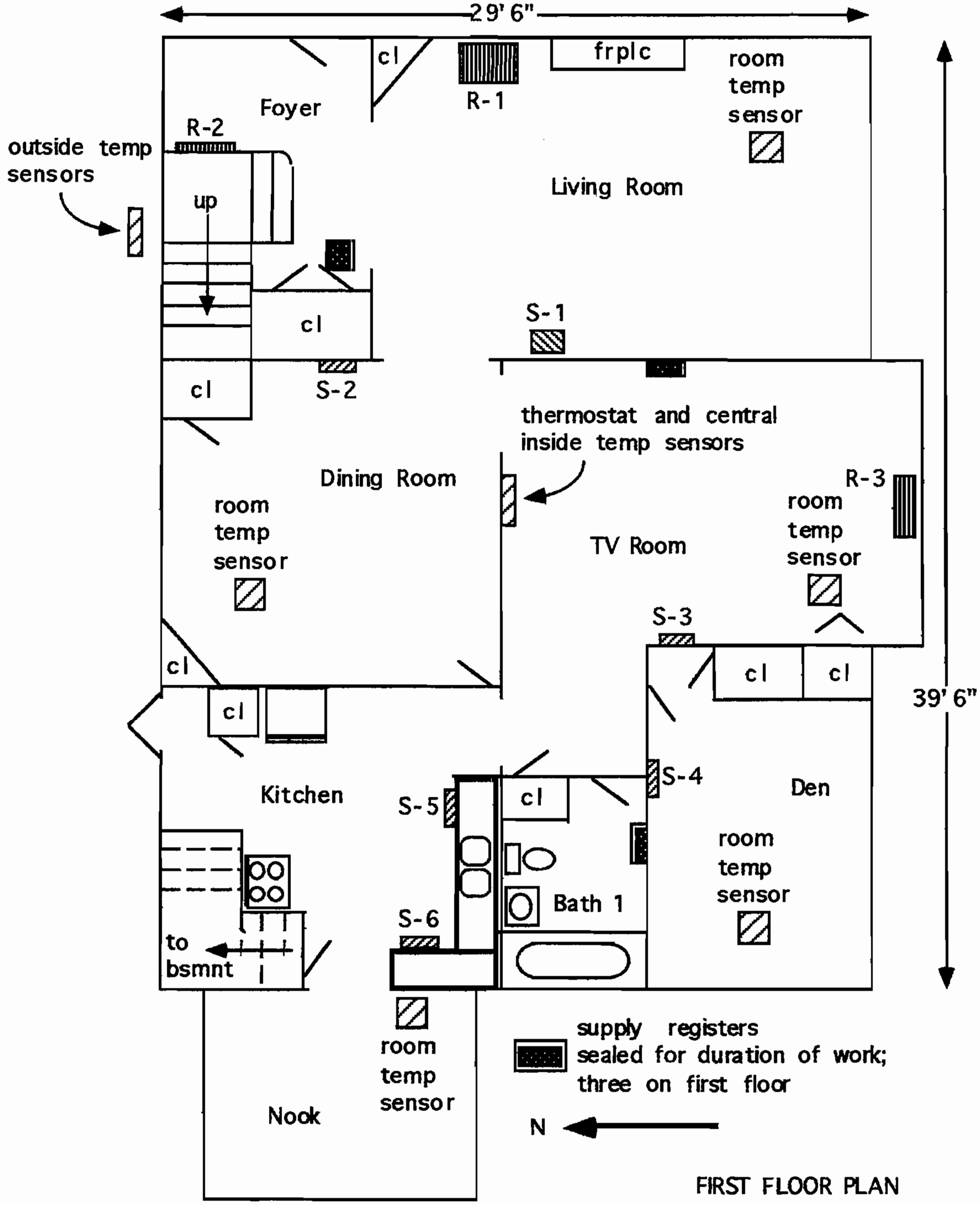
29' 6"
39' 6"
cl
frplc
R-1
room
temp
sensor
Foyer
R-2
outside temp
sensors
up
Living Room
S-1
cl
cl
S-2
thermostat and central
inside temp sensors
Dining Room
R-3
room
temp
sensor
TV Room
room
temp
sensor
S-3
cl
cl
cl
cl
Kitchen
S-5
cl
S-4
Den
room
temp
sensor
Bath 1
S-6
to
bsmnt
room
temp
sensor
Nook
supply registers
sealed for duration of work;
three on first floor
N
FIRST FLOOR PLAN

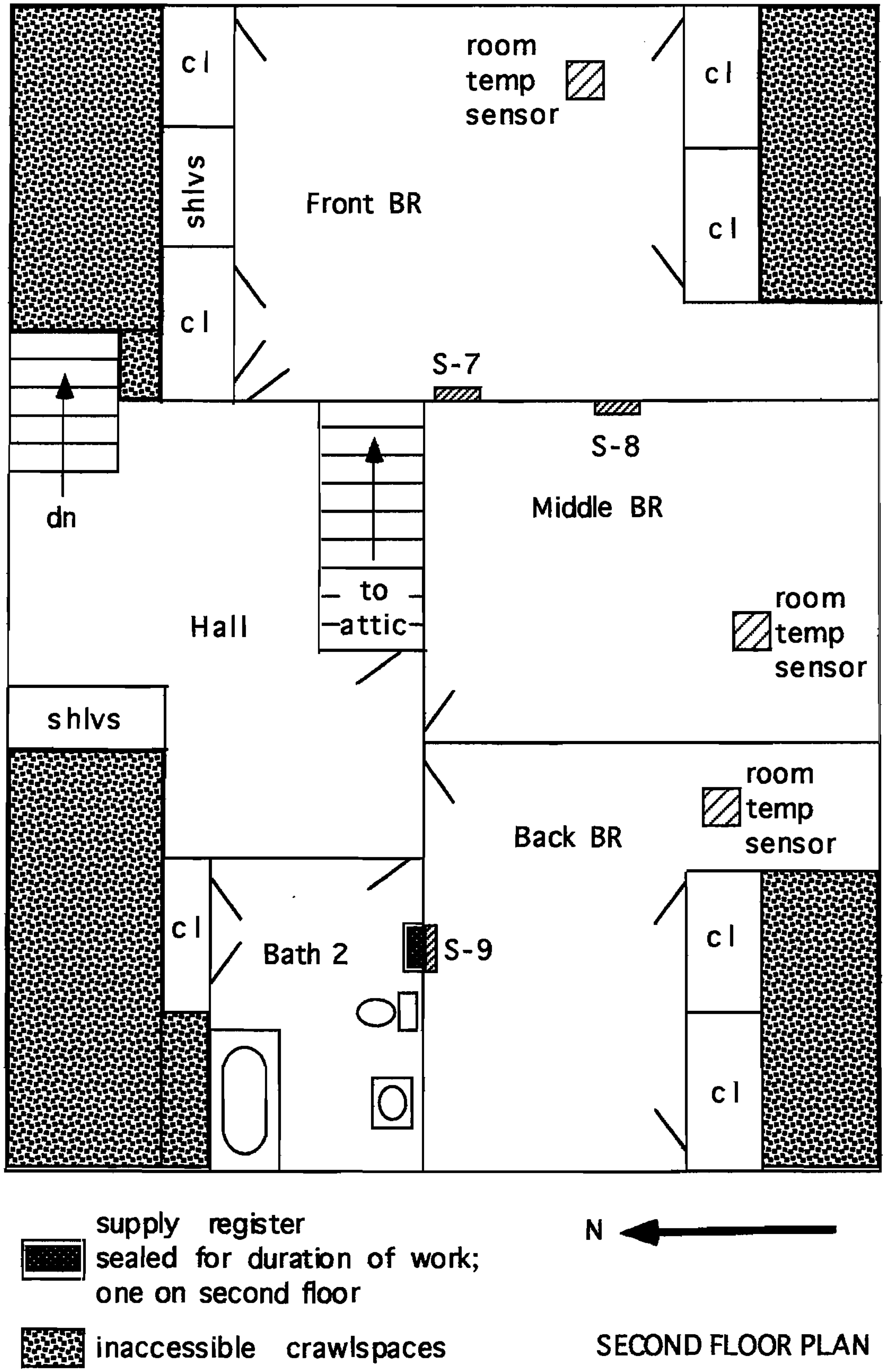


SECOND FLOOR PLAN

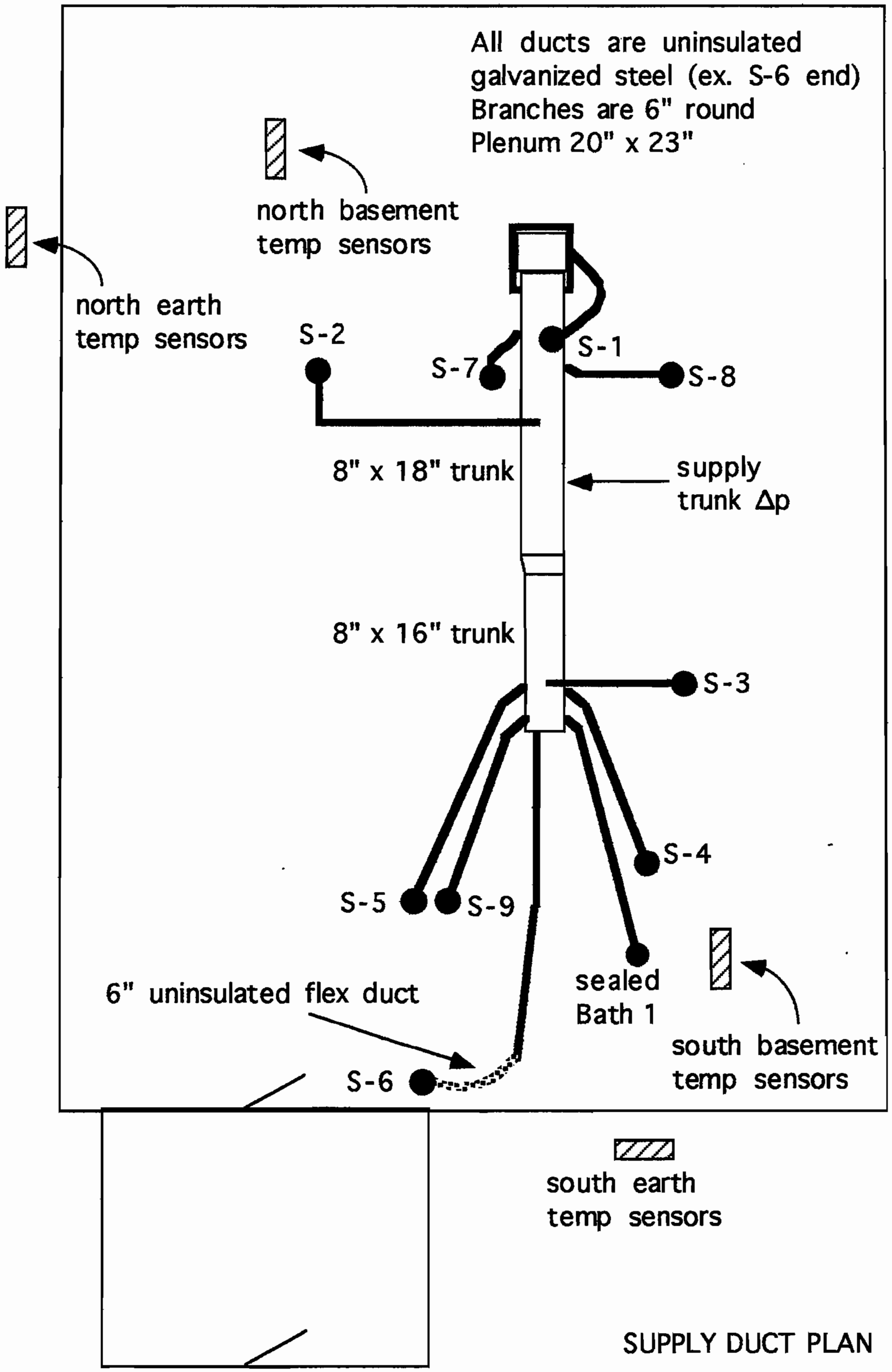


SUPPLY DUCT PLAN

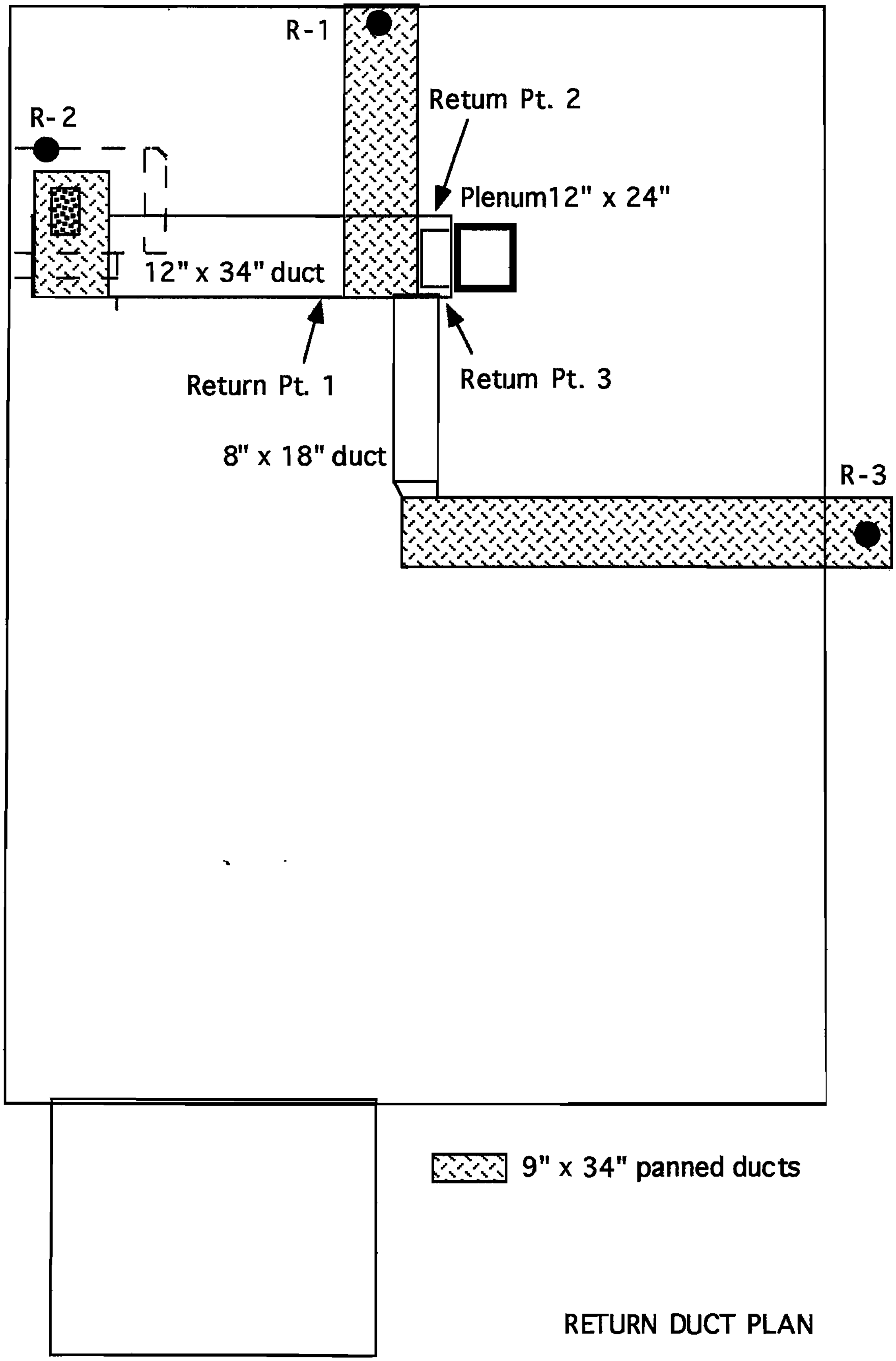


RETURN DUCT PLAN

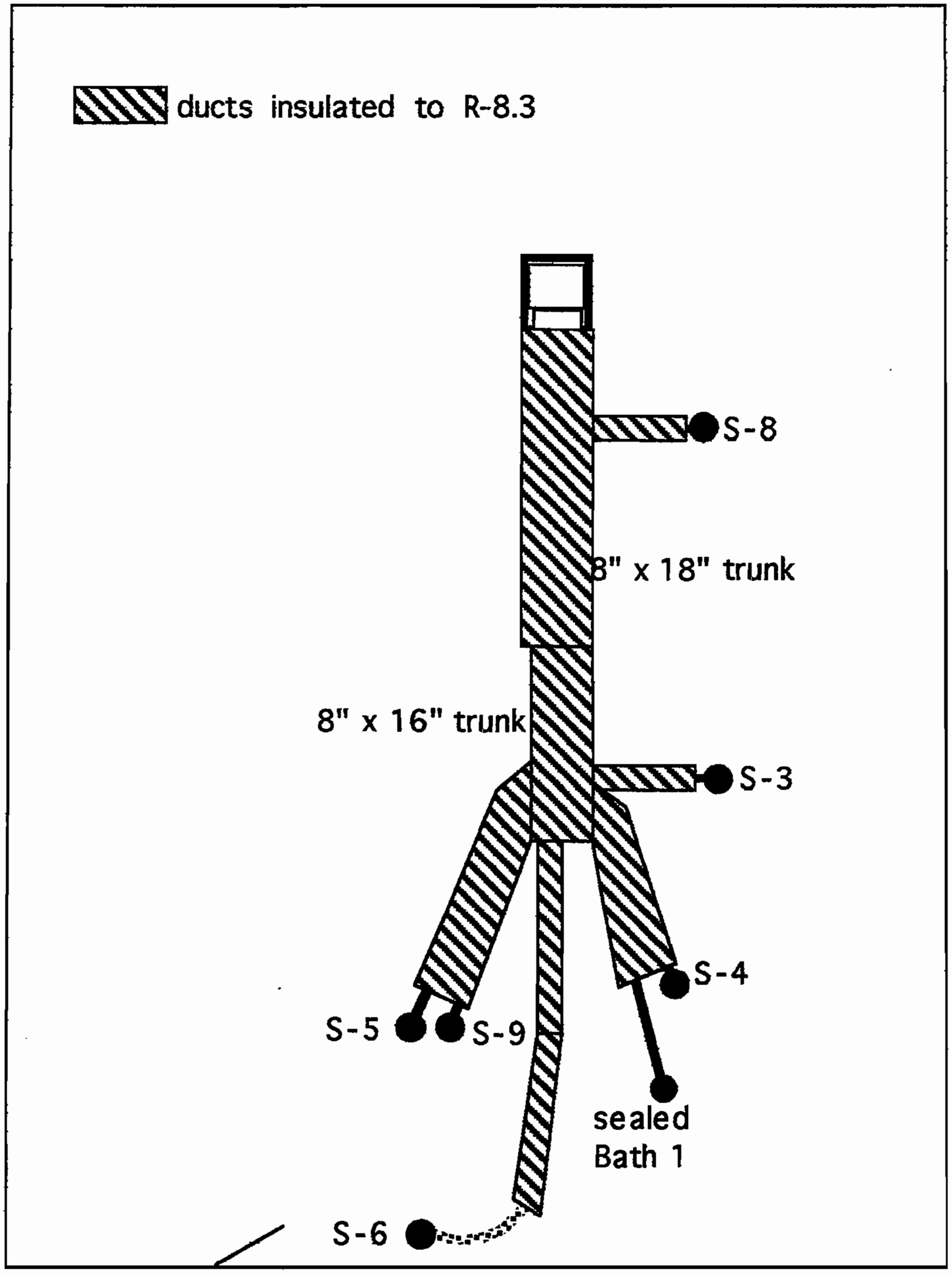


SUPPLY DUCT INSULATION PLAN

# Appendix B
# Uncertainty Analysis

**Estimation of Uncertainty for Absolute Benchmarks for Design or Seasonal Distribution Efficiency**

The uncertainty associated with a predicted value of "y" (here called a benchmark) associated with a new value of "x", using a line which has been fit to a number of data points other than "x", is well-developed in textbooks on statistics, and is repeated here (see References 1-3).

For each furnace cycle, calculated values of distribution efficiency are plotted against indoor-outdoor temperature difference. Linear regression is performed to obtain the best-fit line through these points.

The uncertainties for the predicted values of design and seasonal distribution efficiency are calculated according to the following:

$$\text{Uncertainty} = t * SE(Y_{new})$$

where t = test statistic, taken from a standard statistical table of values of t as a function of both n, the number of data points, and the confidence interval, which is here taken to be 95 percent. For this work, with n ranging from 63 to 138, t is equal to 2.00 or 1.98;

$Y_{new}$ = predicted value of either design or seasonal distribution efficiency; and

$SE(Y_{new})$ = standard error of $Y_{new}$.

$Y_{new}$ and $SE(Y_{new})$ come from the following:

$$Y_{new} = a + b * X_{new}$$

where a = intercept value from the linear regression of distribution efficiency versus indoor-outdoor temperature difference;

b = slope value from the linear regression of distribution efficiency versus indoor-outdoor temperature difference; and

$X_{new}$ = design or seasonal indoor-outdoor temperature difference.

And:

$$SE(Y_{new}) = S * (1 + 1/n + (X_{new} - x_{bar})^2 / SS_{xx})^{0.5}$$

where $S = ((SS_{yy} - b * SS_{xy}) / (n - 2))^{0.5}$;

$x_{bar}$ = mean of x-values (indoor-outdoor temperature differences);

$SS_{xx} = \Sigma(x_i - x_{bar})^2$ ; sum of the squares around the mean of the x-values;

$x_i$ = individual values of x (indoor-outdoor temperature difference) for each data point;

$SS_{yy} = \Sigma(y_i - y_{bar})^2$ ; sum of the squares around the mean of the y-values;

$y_{bar}$ = mean of y-values;

$y_i$ = individual values of y (distribution efficiency) for each data point; and

$SS_{xy} = \Sigma(x_i - x_{bar})^2$ ; sum of the cross product around the means of the x- and y-values.

The predicted uncertainty $t * SE(Y_{new})$ is in units of $Y_{new}$. The following is used to obtain the percent uncertainty:

$$\text{Percent Uncertainty} = 100 * t * SE(Y_{new}) / Y_{new}$$

**Estimation of Uncertainty for Relative Difference Benchmarks for Design or Seasonal Distribution Efficiency**

The first part of the relative difference uncertainty estimation process is identical to the entire distribution efficiency process, except that y-values represent energy consumption rather than distribution efficiency, and data from two different duct configurations is required to generate two different percent uncertainties. Further, here the two predicted y-values are not the benchmarks that are sought; rather their quotient is the benchmark, or the percentage difference between the two. Thus the ultimate percent uncertainty that is sought is not either of the two individual percent uncertainties, but rather the percent uncertainty in the quotient.

For each furnace cycle, values of energy consumption are plotted against indoor-outdoor temperature difference. Linear regression is performed to obtain the best-fit line through these points.

The uncertainties for the predicted values of design and seasonal energy consumption are calculated according to the following: